
Electronic Thesis and Dissertation Repository

6-22-2018 1:00 PM

Evaluating white matter changes and executive function in rat models of mediodorsal thalamic stroke and neuroinflammation

Jessica Garabon, *The University of Western Ontario*

Supervisor: Whitehead, Shawn N., *The University of Western Ontario*

Co-Supervisor: Allman, Brian L., *The University of Western Ontario*

A thesis submitted in partial fulfillment of the requirements for the Master of Science degree in Neuroscience

© Jessica Garabon 2018

Follow this and additional works at: <https://ir.lib.uwo.ca/etd>



Part of the [Nervous System Diseases Commons](#)

Recommended Citation

Garabon, Jessica, "Evaluating white matter changes and executive function in rat models of mediodorsal thalamic stroke and neuroinflammation" (2018). *Electronic Thesis and Dissertation Repository*. 5417. <https://ir.lib.uwo.ca/etd/5417>

This Dissertation/Thesis is brought to you for free and open access by Scholarship@Western. It has been accepted for inclusion in Electronic Thesis and Dissertation Repository by an authorized administrator of Scholarship@Western. For more information, please contact wlsadmin@uwo.ca.

Abstract

Recent literature has supported a relationship between vascular disease and its role in the progression of cognitive impairment. Previous studies have demonstrated that white matter inflammation (WMI) in the brain is a common pathological outcome following stroke. Moreover, WMI has been shown to be the strongest predictor of cognitive decline following stroke. Finally, previous work in our lab has demonstrated, using a rodent model of striatal stroke, that WMI is correlated with post-stroke cognitive impairment. The current study aimed to further investigate the role of WMI in post-stroke cognitive impairment by utilizing a mediodorsal thalamic (MD) stroke model in the rat as well as a rat model of focal white matter inflammation. MD stroke in the mediodorsal thalamus was produced using an injection of the potent vasoconstrictor endothelin-1. Focal WMI was produced using injections of lipopolysaccharide into the corpus callosum. Behavioural flexibility was assessed using an operant set-shifting task to examine executive function, followed by post-mortem immunohistological analyses to assess WMI. We found that unilateral MD stroke produced a regressive behavioural phenotype, however no WMI was observed. Additionally, it was found that LPS-injected rats did not display traditional measures of behavioural inflexibility, however impairment was observed when assessing group error rates using a logarithmic regression model. The MD stroke model findings suggest that young rats may be more resilient to WMI than older rats. Additionally, the LPS model findings suggest that WMI may be implicated in causing executive dysfunction. Finally, this suggests a potential implication for anti-inflammatory treatment in the attenuation of cognitive impairment.

Acknowledgements

First are foremost, I would like to thank my supervisors Dr. Shawn Whitehead and Dr. Brian Allman for their continuous guidance and support throughout the duration of my degree. Their mentorship has shaped me into the researcher that I am today. I would also like to thank my committee members Dr. Raj Rajakumar and Dr. Susanne Schmid for their input and direction in project development.

I have extraordinary gratitude for Dr. Lynn Wang in her teaching and assistance in technical skills throughout my time in the lab. Her expertise truly allowed me to succeed in completing my experiments. I would also like to thank Megha Verma and Jessica Jung for their assistance in tissue sectioning and analysis. Thank you to Bailey Whitehead, Victoria Thorburn, Alex Levit, Fan Liu, Victoria Jaremek, Aaron Harris, Sarah Caughlin, Nadia Ivanova, Mona Alshaikh and Asmahan Elsariti for their friendship and for making the lab such an incredible place to do research. Thank you to Dr. Brittany Balint for your guidance and encouragement throughout this degree. A special thanks to Austyn Roseborough for her writing dates and imparting her love of vegan food on me; I am extremely thankful for your friendship.

I cannot begin to express the gratitude that I have for my family for the love and support they have provided me throughout my life and especially my academic career. I would like to give a special thanks to Camillia DiPasquale for her friendship and support. Finally, I would like to thank my husband Justin Garabon for always providing his unconditional love, guidance and reassurance. I am so thankful to be able to do life with you.

Table of Contents

ABSTRACT.....	I
ACKNOWLEDGEMENTS.....	II
LIST OF FIGURES.....	V
ABBREVIATIONS LIST.....	VI
SECTION 1: INTRODUCTION.....	1
1.1 STROKE IN CANADA	2
1.2 OVERVIEW OF STROKE TYPES.....	2
1.3 PATHOPHYSIOLOGY OF ISCHEMIC STROKE	4
1.4 ASTROCYTE RESPONSE POST-STROKE	8
1.5 MICROGLIA RESPONSE POST-STROKE.....	9
1.6 WHITE MATTER.....	10
1.7 WHITE MATTER INFLAMMATION	11
1.8 COGNITIVE IMPAIRMENT AND EXECUTIVE FUNCTION.....	13
1.9 BEHAVIOURAL FLEXIBILITY AS A MEASURE OF EXECUTIVE FUNCTION.....	14
1.10 RODENT MODELS OF ISCHEMIC STROKE	16
1.11 RODENT MODELS OF WMI.....	18
1.12 RATIONALE, OBJECTIVE, AND HYPOTHESIS – AIM 1	19
1.13 RATIONALE, OBJECTIVE, AND HYPOTHESIS – AIM 2	20
SECTION 2: METHODS.....	22
2.1 ANIMALS	23
2.2 ENDOTHELIN-1 FOCAL ISCHEMIA MODEL	23
2.3 LIPOPOLYSACCHARIDE INJECTIONS	24
2.4 BEHAVIOURAL TESTING	24
2.4.1 STRATEGY SET-SHIFTING	24
2.4.1.1 FOOD RESTRICTION	27
2.4.1.2 APPARATUS	27
2.4.1.3 TRAINING	29
2.4.1.4 SIDE BIAS DETERMINATION	30
2.4.1.5 VISUAL CUE DISCRIMINATION TESTING.....	30
2.4.1.6 RESPONSE DISCRIMINATION SET-SHIFT TESTING.....	31
2.4.1.7 RESPONSE DISCRIMINATION REINFORCEMENT.....	31
2.4.1.8 INTRADIMENSIONAL REVERSAL TESTING	32
2.4.1.9 ERROR ANALYSIS	32
2.4.2 MORRIS WATER MAZE	33
2.4.2.1 APPARATUS	33
2.4.2.2 LEARNING TRIALS	34
2.4.2.3 RETENTION PROBE TESTING	34
2.4.2.4 VISUAL CUE TESTING.....	35
2.5 TISSUE COLLECTION AND PREPARATION	36
2.6 THIONIN HISTOCHEMISTRY	36
2.7 IMMUNOHISTOCHEMISTRY	37
2.8 MICROSCOPY IMAGING AND ANALYSIS	38
2.9 STATISTICAL ANALYSIS.....	38
SECTION 3: RESULTS.....	40

3.1	BEHAVIOURAL ASSESSMENTS – AIM 1	41
3.1.1	RAW METRICS OF INITIAL DISCRIMINATION LEARNING ARE NOT AFFECTED FOLLOWING MD STROKE	41
3.1.2	RAW METRICS OF SET-SHIFTING ARE NOT AFFECTED FOLLOWING MD STROKE	41
3.1.3	ERROR PROFILE SUGGESTS MILD IMPAIRMENT BEHAVIOURAL FLEXIBILITY FOLLOWING MD STROKE	44
3.1.4	MODELLING LOGISTIC REGRESSION OF INCONGRUENT TRIAL ERROR RATES FOLLOWING MD STROKE.....	46
3.2	HISTOCHEMISTRY AND IMMUNOHISTOCHEMISTRY – AIM 1	46
3.2.1	THIONIN, NEUN AND OX-6 ANALYSIS OF ET-1 INJECTION SITE(S)	46
3.2.2	NO GROUP DIFFERENCE IN MICROGLIOSIS OR ASTROGLIOSIS IN THE CORPUS CALLOSUM FOLLOWING MD STROKE 49	
3.2.3	NO GROUP DIFFERENCE IN MICROGLIOSIS OR ASTROGLIOSIS IN FORCEPS MINOR FOLLOWING MD STROKE 49	
3.2.4	NO NEURONAL LOSS IN PFC OR NAC FOLLOWING MD STROKE	52
3.3	BEHAVIOURAL ASSESSMENTS – AIM 2	52
3.3.1	INITIAL DISCRIMINATION LEARNING NOT AFFECTED BUT MEMORY FOR INITIAL STRATEGY SLIGHTLY IMPAIRED FOLLOWING LPS INJECTIONS	52
3.3.2	RAW METRICS OF SET-SHIFTING ARE NOT AFFECTED FOLLOWING LPS INJECTIONS.....	54
3.3.3	ERROR PROFILE SUGGESTS NO IMPAIRMENT IN BEHAVIOURAL FLEXIBILITY FOLLOWING LPS INJECTIONS .	54
3.3.4	MODELLING LOGISTIC REGRESSION OF INCONGRUENT TRIAL ERROR RATES FOLLOWING LPS INJECTIONS .	57
3.3.5	SPATIAL NAVIGATION AND MEMORY NOT AFFECTED FOLLOWING LPS INJECTIONS	57
3.4	HISTOCHEMISTRY AND IMMUNOHISTOCHEMISTRY – AIM 2.....	61
3.4.1	LPS RATS HAD SIGNIFICANTLY INCREASED MICROGLIOSIS AND ASTROGLIOSIS IN CORPUS CALLOSUM.....	61
3.4.2	LPS RATS HAD SIGNIFICANTLY INCREASED MICROGLIOSIS BUT NOT ASTROGLIOSIS IN FORCEPS MINOR.....	61
SECTION 4: DISCUSSION.....		65
4.1	UNILATERAL MD STROKE RATS DISPLAYED MILD BEHAVIOURAL INFLEXIBILITY IN THE FORM OF A REGRESSIVE PHENOTYPE	66
4.2	MD STROKE RATS DID NOT DISPLAY WMI OR CELL LOSS IN AREAS OF CONNECTED CIRCUITRY MEDIATING BEHAVIOURAL FLEXIBILITY	68
4.3	LPS-INJECTED RATS DISPLAYED MILD IMPAIRMENT IN BEHAVIOURAL FLEXIBILITY IN ADDITION TO SIGNIFICANT WMI	69
4.4	CAVEATS AND FUTURE DIRECTIONS.....	72
SECTION 5: SUMMARY AND CONCLUSIONS.....		75
REFERENCES.....		78
<i>CURRICULUM VITAE.....</i>		98

List of Figures

Figure 1.1: The general progression of post-stroke inflammation.....	5
Figure 1.2: Neural circuitry mediating specific components of behavioural flexibility.....	15
Figure 2.1: Surgical and behavioural timeline for ET-1 study.....	25
Figure 2.2: Surgical and behavioural timeline for LPS study.....	26
Figure 2.3: Set-shifting behavioural task apparatus and strategies.....	28
Figure 3.1: Raw metrics of initial discrimination learning are not affected following MD stroke.....	42
Figure 3.2: Raw metrics of set-shifting are not affected following MD stroke.....	43
Figure 3.3: Error profile suggests mild impairment in behavioural flexibility following MD stroke.....	45
Figure 3.4: Modelling logistic regression of incongruent trial error rates following MD stroke.....	47
Figure 3.5: Thionin, NeuN and OX-6 analysis of ET-1 injection site(s).....	48
Figure 3.6: No group difference in microgliosis or astrogliosis in the corpus callosum following MD stroke.....	50
Figure 3.7: No group difference in microgliosis or astrogliosis in the forceps minor following MD stroke.....	51
Figure 3.8: No neuronal loss in PFC or NAc following MD stroke.....	53
Figure 3.9: Initial discrimination learning not affected but memory for initial strategy slightly impaired following LPS injections.....	55
Figure 3.10: Raw metrics of set-shifting are not affected following LPS injections.....	56
Figure 3.11: Error profile suggests no impairment in behavioural flexibility following LPS injections.....	58
Figure 3.12: Modelling logistic regression of incongruent trial errors rates following LPS injections.....	59
Figure 3.13: Spatial navigation and memory not affected following LPS injections.....	60
Figure 3.14: LPS rats displayed increased microgliosis and astrogliosis in the corpus callosum.....	62
Figure 3.15: LPS rats displayed increased microgliosis but not astrogliosis in the forceps minor.....	64

Abbreviations List

AMPA	α -amino-3-hydroxy-5-methyl-4-isoxazolepropionic acid
ANOVA	Analysis of variance
BBB	Blood-brain barrier
Bcl-2	B-cell lymphoma-2
CAMs	Cellular adhesion molecules
CC	Corpus callosum
CCR5	CC chemokine ligand-5
CNS	Central nervous system
CNTF	Ciliary neurotrophic factor
DAB	3-3-diaminobenzene tetrahydrochloride
ddH₂O	Double-distilled water
dsRNA	Double-stranded ribonucleic acid
ED	Executive dysfunction
ET-1	Endothelin-1
G-CSF	Granulocyte-colony stimulating factor
GFAP	Glial fibrillary acidic protein
HMG-1	High mobility group protein-1
HSP-70	Heat shock protein-70
ICAM-1	Intercellular adhesion molecule-1
IGF-1	Insulin-like growth factor
IL-1	Interleukin-1
IL-6	Interleukin-6
IL-8	Interleukin-8
IL-10	Interleukin-10
iNOS	Inducible nitric oxide synthase
IV	Intravenous
LPS	Lipopolysaccharide
MCAO	Middle cerebral artery occlusion

MCP-1	Monocyte chemoattractant protein-1
MD	Mediodorsal thalamus
MHC-II	Major histocompatibility complex II
MMP-9	Matrix metalloprotease-9
MMP	Matrix metalloprotease
MWM	Morris water maze
NAc	Nucleus accumbens
NE	Northeast
NeuN	Neuronal nuclei
NMDA	N-methyl-D-aspartate
NOS	Nitric oxide species
NRE	Never-reinforced error
NT-3	Neurotrophin-3
NW	Northwest
PBS	Phosphate buffered saline
PET	Positron emission tomography
PFA	Paraformaldehyde
PFC	Prefrontal cortex
PrPc	Prion protein
RANTES	Regulated on activation normal T-cell expressed and secreted
RD	Response discrimination
ROS	Reactive oxygen species
siRNA	Small interfering ribonucleic acid
SE	Southeast
SEM	Standard error of the mean
SW	Southwest
TGF-β	Transforming growth factor- β
TNF-α	Tumor necrosis factor- α
VCAM-1	Vascular adhesion molecule-1
VD	Visual cue discrimination

VEGF	Vascular endothelial growth factor
WCST	Wisconsin Card Sorting Task
WMI	White matter inflammation
WT	Wildtype

Section 1: INTRODUCTION

1.1 Stroke in Canada

Stroke is the third most frequent cause of mortality in Canada ¹. In 2013, a total of 741,800 Canadians had experienced a stroke or were living with the effects of a previous stroke, and 57,040 Canadians died from a stroke ¹. Many factors can increase the risk of stroke, including hypertension, smoking, diabetes, dyslipidemia, obesity and atrial fibrillation ²⁻⁵. A person's risk of suffering a stroke also increases rapidly with age, making it a significant health issue given the increasingly aging population in Canada ¹. More recently, a trend towards decrease incidence of stroke has been observed, likely due to the increase in awareness of risk factors associated with stroke ¹. For example, prevention efforts commonly include maintaining aspects of a healthy lifestyle including having a healthy diet, regular exercise regimen, avoiding alcohol and smoking, and controlling certain physiological conditions such as hypertension. Despite this recent decrease in incidence, better understanding of the molecular mechanisms of stroke damage is still required to improve recovery post-stroke.

1.2 Overview of stroke types

There are two major categories of stroke: hemorrhagic and ischemic. Hemorrhagic strokes occur when blood is released into the brain as a result of a vessel rupture within the brain and accounts for approximately 13% of observed strokes. The released blood causes an increase in pressure and damage to the affected brain region ⁶. Alternatively, ischemic strokes occur when a blockage of a cerebral blood vessel results in hypoperfusion, or complete blockage, of blood to an area of the brain, causing hypoxia, hypoglycemia and neurodegeneration in that region ⁷. Ischemic strokes are much more prevalent, accounting for approximately 87% of all observed strokes ⁸. There are three sub-classifications of ischemic stroke. The first type is thrombotic,

which is mainly caused when an atherosclerotic process initiates the formation of a thrombus at a particular location along the vessel, restricting blood flow to downstream vessel branches and brain structures. Other causes of thrombotic stroke include trauma or hemostatic disorders/disturbances ⁹. Another type of ischemic stroke is embolic stroke, in which a blood clot is formed in a different region of the body, such as the heart or extremities, and subsequently travels through the vasculature into a cranial artery where it becomes lodged, thus restricting blood flow past that point ¹⁰. Embolic strokes are more likely to occur in individuals with atrial fibrillation, as this condition causes a thrombus to form within the heart, which could be transferred into the cerebral vasculature ¹¹. The last subtype is the lacunar stroke, which is not specified based on the process of vessel blockage, but rather the size of the vessel it affects. When an infarct occurs in a small vessel within the brain, it is called a lacunar stroke. A lacunar stroke accounts for approximately one quarter of ischemic strokes and it affects structures that are found deep within the brain, such as the basal ganglia, thalamus, internal capsule and brainstem ^{12,13}. Lacunar strokes are also known as “silent strokes” since they may not elicit a clinically appreciable response upon occurrence but can cause very subtle deficits that accumulate over time ¹⁴. Risk factors for lacunar stroke include diabetes, smoking and hypertension ¹⁵. Conversely, cardiologic diseases such as atherosclerosis and atrial fibrillation are not risk factors for lacunar stroke as the etiology of lacunar strokes is not the same as the typical thrombotic and embolic stroke^{15,16}. Additionally, the occurrence of a lacunar stroke increases the risk that a subsequent stroke will occur and it also increase the risk for post-stroke cognitive impairment ¹⁴. Given the associated risk of lacunar stroke and cognitive impairment, work in this thesis will focus on a pre-clinical model of lacunar stroke.

1.3 Pathophysiology of ischemic stroke

The cellular events that occur following an ischemic stroke play a large role in the progression of cerebral damage (Figure 1.1) ¹⁷. When perfusion to an area of the brain is initially reduced there is a specific inner core region that experiences severe ischemia. Following 5-10 minutes without adequate perfusion, this ischemic region becomes necrotic as the composing neurons and glia die due to excitotoxicity ¹⁰. Outside this core region is an area that experiences less severe ischemia due to small amounts of supportive collateral blood supply. This region, called the penumbra, may still maintain viability if appropriate therapeutic measures are delivered in time ¹⁸. In this region, cells can initiate apoptosis through the intrinsic apoptotic pathway, extrinsic apoptotic pathway and various other sequences that ultimately result in cell death ¹⁰.

In the acute phase following a stroke (minutes to hours), cells that experience hypoxia initiate a complex cascade of processes that involve effects ranging from cellular communication to structural changes in the tissue ¹⁹. Brain tissue can become damaged when it is no longer receiving oxygen, resulting in a depletion of ATP. Brain tissue can also be damaged if it undergoes a period of hypoxia and is rapidly reperfused. When cells become damaged, they lose membrane ion transporter function, causing a disruption in the ionic gradient ²⁰. This results in cytotoxic edema resulting in increased permeability of cerebral blood vessels, which causes an influx of large serum proteins that draw in water ²⁰.

The progression of cellular death can also occur when damaged neurons begin to release excitatory neurotransmitters such as glutamate and aspartate. These neurotransmitters can over-activate N-methyl-D-aspartate (NMDA) and α -amino-3-hydroxy-5-methyl-4-isoxazolepropionic

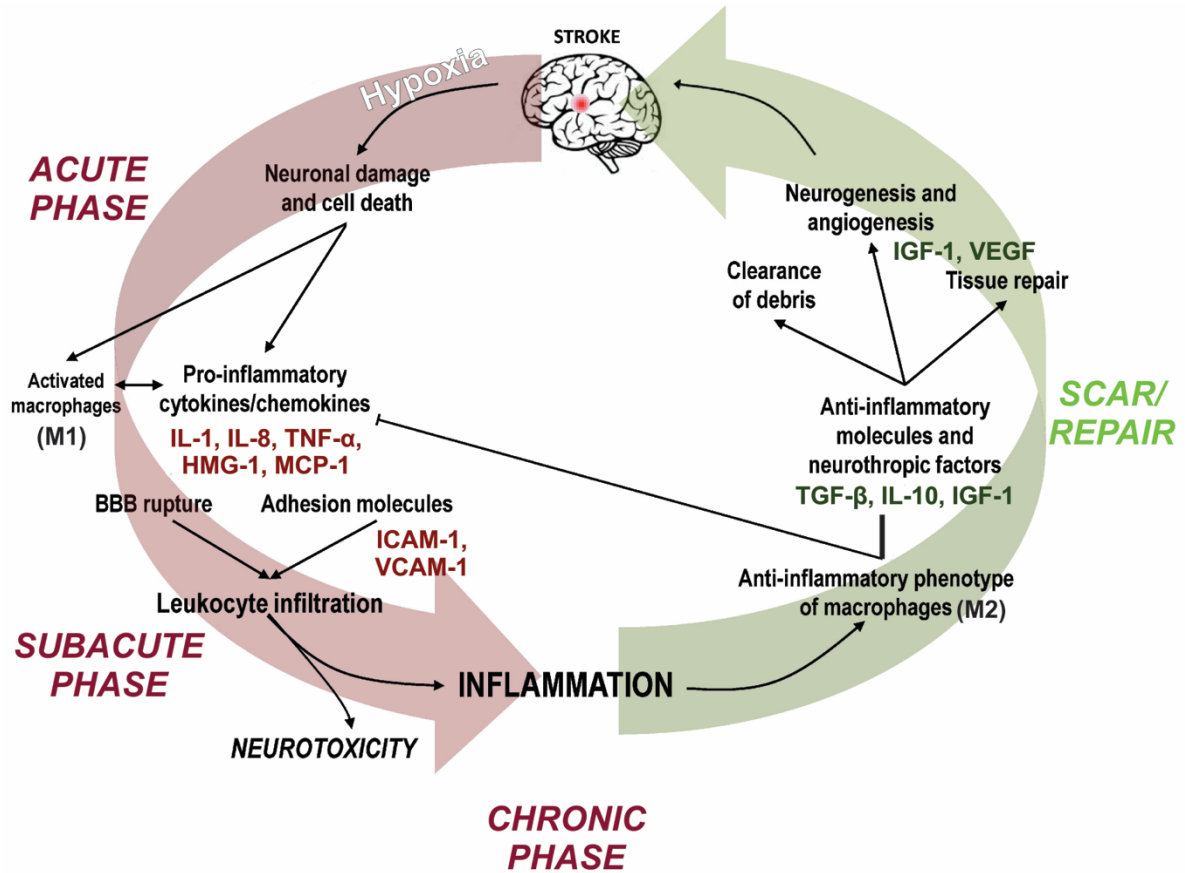


Figure 1.1: The general progression of post-stroke inflammation. The acute phase following a stroke involves hypoxia that causes cell death and damage. This results in the release of various pro-inflammatory mediators and the activation of immune cells such as macrophages or microglia. In the subacute phase, the disrupted blood-brain barrier and adhesion molecules produced lead to the infiltration of more leukocytes to propagate inflammation. As the inflammation becomes chronic, anti-inflammatory molecules and cellular processes become predominant and the scar/healing process begins. This includes reparative processes, removal of cellular debris and tissue repair. Adapted from: Simats, Garcia-Berrocso and Montaner (2015).

acid (AMPA) receptors, causing enzymatic dysregulation resulting in subsequent cellular degradation ²¹. In addition to excitatory neurotransmitters, damaged cells also produce reactive oxygen species (ROS) and free radicals, both of which induce cellular damage and initiate apoptosis. The production of ROS also result in the activation of matrix metalloproteases (MMPs), which alter the structural integrity of the brain by breaking down the blood-brain barrier (BBB) ²². In the acute phase, this is specifically accomplished by MMP-9 ²³.

Ischemia can be further exacerbated through vascular dysregulation and nitric oxide species (NOS) production. Following ischemia, endothelin receptors are upregulated ²⁴.

Endothelin is a mediator of vascular smooth muscle contraction leading to vasoconstriction, reducing perfusion to the ischemic area ²⁴. This process may be counteracted with vasodilation caused by NOS released from ischemic induced endothelial cells. Conversely, neurons and immune cells in the ischemic area will also produce NOS, but this product will exacerbate cellular damage when produced from these cell types by increasing levels of ROS ²⁵.

Neuropeptides are also upregulated post-stroke and play a role in ROS production and vascular dysregulation. For example, increases in Substance P post-stroke results in additional inflammatory cytokine upregulation and free radical release, but it also promotes vasodilation through the promotion of NOS from endothelial cells ²⁶. Neuropeptide Y also causes an increase in the production of NOS from endothelial cells and neurons ¹⁰. Altogether, vascular dysregulation and increases in neuropeptide release all increase ROS production, further exacerbating brain damage in the ischemic area.

Inflammation plays a critical role in the pathogenic processes of stroke. Injured cells affected by ischemia produce inflammatory mediators such as cytokines and chemokines, which recruit additional immune cells to potentiate the inflammatory response. These inflammatory

mediators are released by neurons, endothelial cells within vessel walls or primarily glial cells such as astrocytes and microglia. Proinflammatory cytokines produced by these cells include interleukin-1 (IL-1), tumor necrosis factor- α (TNF- α) and high mobility group protein-1 (HMG-1) ²⁷⁻²⁹. Proinflammatory cytokines and chemokines are upregulated post-stroke with the purpose of attracting additional peripheral immune cells into the brain. These include interleukin-8 (IL-8) for neutrophil recruitment, monocyte chemoattractant protein-1 (MCP-1) for monocyte recruitment, CC chemokine ligand-5 (CCR5) and regulated on activation normal T-cell expressed and secreted (RANTES) ^{27,30,31}. All together the upregulation of these pro-inflammatory molecules potentiate the current inflammation that occurs post-stroke.

Some anti-inflammatory compounds are also produced in the acute phase following a stroke. These include transforming growth factor- β (TGF- β) and interleukin-10 (IL-10) ^{32,33}. Other neuroprotective factors produced during the acute phase are heat shock protein-70 (HSP-70), B-cell lymphoma-2 (Bcl-2) family proteins, prion protein (PrPc), neurotrophin-3 (NT-3) and granulocyte-colony stimulating factor (G-CSF) ³⁴⁻³⁷. These anti-inflammatory mediators are important for the initial control of the inflammatory response following a stroke.

In the subacute phase (hours to days) following a stroke, cells of the immune system begin to play a significant role in post-stroke inflammatory processes. Pro-inflammatory mediators produced in the subacute phase will initiate the upregulation of cellular adhesion molecules (CAMs) such as intercellular adhesion molecule-1 (ICAM-1) and vascular adhesion molecule-1 (VCAM-1) ^{38,39}. These molecules allow circulating peripheral leukocytes to attach to the endothelium of the vasculature and subsequently infiltrate into the adjacent cerebral tissue ⁴⁰. The introduction of these immune cells will allow for further propagation of inflammatory mediators and MMP activation. The production of various vascular growth factors by the newly

infiltrated immune cells helps to create angiogenesis in response to the brain damage that has been caused ⁴¹.

In the chronic period after a stroke has taken place (days to months), the inflammatory mediators cause upregulation of apoptotic gene expression ⁴². Harmful processes subside due to the removal of cell debris, the production of anti-inflammatory factors and the production of pro-survival and growth factors ^{43,44}. Cell debris removal is accomplished by microglia and infiltrating macrophages ^{45,46}. Anti-inflammatory factors such as TGF- β and IL-10 are produced by microglia and regulatory T-cells, respectively ^{32,47}. Lastly, neurons, microglia, astrocytes and other inflammatory cells all participate in repair by producing growth factors such as insulin-like growth factor 1 (IGF-1) and vascular endothelial growth factor (VEGF) in order to promote neuron sprouting, neuron regeneration, angiogenesis, etc. ⁴⁸⁻⁵¹. Ultimately, the inflammatory components involved in the chronic phase following a stroke are focused on repairing damaged tissue and developing a scar around the affected area ^{52,53}.

1.4 Astrocyte response post-stroke

Astrocytes have a critical role in maintaining neuronal health and are required for neuron survival. Part of the blood-brain barrier (BBB) is formed by astrocytic processes that form tight junctions with capillaries in the brain ⁵⁴. The proximity of these processes to cerebral capillaries create an important role for astrocytes for water balance within the brain. When edema occurs following a stroke, these processes are the first to become edematous as they contain a large amount of aquaporins that allow for water regulation ^{55,56}. Within hours following a stroke ‘reactive astrogliosis’ occurs, meaning astrocytes become hypertrophic and proliferate at the site of damage ⁵⁷. These cells are more protected, relative to neurons, in the setting of ischemia as

they are not impacted by glutamate cytotoxicity and are generally more adaptive during hypoxia^{58,59}. Reactive astrocytes will also upregulate structural proteins such as glial fibrillary acidic protein (GFAP), which is a critical component of the astrocyte cytoskeleton and is also thought to be involved with signalling and cellular behaviour in periods of stress⁶⁰. In the acute setting to days following a stroke, these reactive cells can produce cytokines, chemokines and interferons⁶¹⁻⁶⁴. Reactive astrocytes are also involved in the healing process following a stroke and form a 'glial scar' surrounding the damaged area of the brain. This scar is created with intertwined astrocyte processes, GFAP, collagen and proteoglycans and it blocks regenerating axons^{65,66}. MMPs are also produced by reactive astrocytes, which contribute to BBB remodelling and repair^{67,68}. Lastly, astrocytes also assist with neurite growth and neurogenesis via the production of trophic factors such as IGF-1 and ciliary neurotrophic factor (CNTF)⁵⁷. Overall, astrocytes have a critical role in propagating an inflammatory response following a stroke and continue to participate in scar formation and neural repair long after an ischemic event.

1.5 Microglia response post-stroke

Microglia play a critical role in the brain following a stroke, but the various presentations of these cells cause their role in stroke pathophysiology to be complex. In the healthy brain, microglia function to survey the brain environment⁶⁹. Following stroke, inflammatory mediators such as monocyte chemoattractant protein-1 (MCP-1) are released from degenerating neurons which act as chemoattractants for microglia recruitment to the ischemia region^{70,71}. Following recruitment, microglia generally show characteristics of an M1 or M2 phenotype. The activation status is complex and relies on a variety of factors, but mostly depend on the timing post-stroke.

⁷². M1 microglia are recruited early to the ischemic site post stroke and play a role in pro-inflammatory processes. by releasing ROS, NOS and proinflammatory cytokines such as IL-1, TNF- α and interleukin-6 (IL-6); all of which cause neuronal death ^{73,74}. They also produce MMPs that further contribute to the destruction of the BBB resulting in subsequent leukocyte infiltration. Alternatively, M2 microglia are considered anti-inflammatory as they release anti-inflammatory cytokines and mediators such as TGF- β , VEGF and IL-10 ^{39,75-77}. M2 microglia are recruited later in the post-stroke process and play a role in tissue repair and angiogenesis ^{76,77}. Overall, microglia can serve drastically different functions over the post-stroke period and are critical to both the damage and repair that occurs.

1.6 White matter

The brain is composed of both grey matter and white matter. Grey matter comprises the cell bodies of neurons, along with their axon terminals and dendrites. White matter contains the axons of neurons which form tracts to form the connection between grey matter structures allowing for communication between areas of the brain ⁷⁸. Axons within the white matter are surrounded by myelin, a lipid-rich substance that provides electrical insulation to axons, allowing for faster conduction of action potentials. In the central nervous system (CNS), myelin is produced by oligodendrocytes ⁷⁹. There are three overarching categories of white matter tracts: (1) projection fibers, (2) association fibers and (3) commissural fibers, which each serve a different function ⁷⁸. Projection fibers connect subcortical areas of the brain to areas within the cortex, while association fibers connect regions of the cortex to other areas within the ipsilateral hemisphere ⁷⁸. Finally, commissural fibers connect corresponding areas of the ipsilateral and contralateral hemispheres ⁷⁸.

White matter is disproportionately hypoperfused in comparison to grey matter and is thus highly susceptible to damage when exposed to reduced blood flow⁸⁰. Energy metabolism in axons occurs independently from neuron cell bodies, therefore, if energy supply is disrupted at any point along the axon due to hypoperfusion, axon viability may be compromised¹². Moreover, axonal degeneration can occur without any damage to their neuronal cell body^{81,82}. Damage to the white matter caused by pathological processes including stroke reduces the functionality of white matter circuitry, as the transmission of action potentials is disrupted, which may have negative cognitive outcomes to the affected individual⁸³.

1.7 White matter inflammation

A commonly identified pathological outcome following a stroke is the onset of neuroinflammation. White matter is hypoperfused relative to grey matter, which may contribute to its vulnerability to hypoxia and the resulting inflammatory response that leads to ischemic injury⁸⁴⁻⁸⁶. As previously mentioned, damage and necrosis of brain tissue occurs following stroke as a result of a robust inflammatory reaction marked by production of inflammatory cytokines, passage of peripheral immune cells through the disrupted BBB and activation of microglia and astrocytes. Due to the hypoperfusion of white matter, oligodendrocytes and progenitors are very susceptible to the effects of inflammation caused by stroke, and this leads to continued inflammation within the white matter following ischemia⁸⁷. Approximately 95% of stroke infarcts affect white matter to some degree, and on average, half of the volume of these infarcts is in white matter locations⁸⁸.

Ischemic stroke has been shown to be a reliable cause of white matter inflammation (WMI)^{84,85}. WMI is extremely dynamic and has been shown to spread to remote areas of the

brain following a stroke ^{81,89}. For example, in one clinical study investigating a positron emission tomography (PET) marker for activated microglia, which is used as an indicator of inflammation, it was found that white matter inflammation was seen not only at the point of injury, but also in remote white matter areas of the brain where it continued to persist 6 months following stroke ⁹⁰. Furthermore, there is evidence that remote degeneration from an acute ischemic infarct is facilitated through connecting white matter tracts ^{91,92}. Therefore, an ischemic stroke appears to cause WMI that can propagate to distant regions via white matter structures.

In addition to WMI produced by cerebral injury, levels of WMI will also increase as an individual ages and may be related to a chronic state of hypoperfusion ⁹³. WMI is an identified risk factor for stroke and it strongly affects the outcome of an individual when a stroke has occurred ⁹⁴. In terms of the damage elicited by a stroke, infarct volumes are larger when WMI is present at baseline prior to a stroke ⁹⁵⁻⁹⁷. The presence of WMI prior to a stroke also increases the functional deficits caused by a stroke and a greater extent of inflammation will exacerbate these effects further ^{94,95,98}. Most importantly, the extent of WMI has been shown to be the strongest predictor of post-stroke cognitive impairment ^{84,99}. For example, the prognosis of a stroke patient is greatly affected by preceding WMI, as it is indicative of an unfavourable recovery at three months following a stroke and a greater rate of mortality at one year post-stroke ¹⁰⁰⁻¹⁰². One potential explanation for the negative impact of WMI is the fact that it can alter the structure and function of white matter bundles, likely disturbing the processes involved with plasticity and repair following a stroke ^{103,104}.

1.8 Cognitive impairment and executive function

Recent literature has strongly supported a relationship between vascular disease and the progression of cognitive impairment^{105–108}. Cognitive deficits observed following stroke can be diverse depending on the brain areas impacted by the injury; and this phenomenon has been demonstrated in pre-clinical models of stroke. For example, when a stroke was induced within the motor cortex, rats demonstrated difficulties in completing tasks that require intact motor capabilities. Whereas when a stroke was induced within the hippocampus, rats demonstrated impairments in spatial learning and memory^{109,110}.

A key aspect of cognitive decline post-stroke involves impairment in executive function¹¹¹. Executive functions includes higher order processes such as planning, rule discovery, behavioural flexibility and working memory¹¹², all of which rely on intact white matter connectivity^{113,114}. Injury to these white matter tracts that connect key brain regions can be detrimental to the proper functioning of the circuitry and their gray matter targets. Animal models of focal ischemic stroke targeting specific grey matter structures have been able to reliably produce cognitive impairment in the form of executive dysfunction (ED)^{115,116}. For example, previous experimental work has explored the effects of small striatal infarcts on WMI and executive function. Interestingly, results showed that rats with the greatest amount of inflammation (as denoted by activated microglia) in frontal white matter structures displayed the greatest degree of behavioural inflexibility, a correlate of ED (preliminary data). This, together with clinical evidence, suggests that WMI and ED may occur concomitantly.

1.9 Behavioural flexibility as a measure of executive function

A component of executive function often disrupted following stroke is behavioural flexibility, which is defined as the ability to alter behaviour in response to changing environmental stimuli ¹¹⁷. It involves a number of higher order functions including generating novel behavioural strategies and maintaining these strategies while suppressing the use of previously successful strategies ¹¹⁸. Behavioural flexibility, along with the other domains of executive function, depends highly on the integration of multiple brain structures, which relies on functional white matter connectivity ^{113,114}. Behavioural flexibility has been commonly assessed clinically using the Wisconsin Card Sorting Task (WCST) ¹¹⁷. Using animal models of disease to assess clinical questions in humans presents a need to develop adequate behavioral testing paradigms for behavioural flexibility in animal models.

There have been several tests of ED that incorporate aspects of behavioural flexibility for rodents. Through the use of these tests, the neural circuitry mediating behavioural flexibility has been identified using pharmacological inactivation approaches, and are comprised of the prefrontal cortex (PFC), nucleus accumbens (NAc) and mediodorsal thalamus (MD) ¹¹⁸ (Figure 1.2). Circuitry connecting the PFC and MD have been shown to regulate strategy shifting from an old to new paradigm ¹¹⁸. Damage to this circuitry in rats resulted in impairments in the ability to switch to a new strategy indicated by perseverative behaviours ¹¹⁸. Circuitry connecting the MD to the NAc is shown to be involved in regulating the use of unrewarding or inappropriate strategies ¹¹⁸. Damage to this connection in rats resulted in an increase in strategy exploration and ‘guessing’ errors ¹¹⁸. Finally, PFC and NAc circuitry is associated with maintaining the use of a novel strategy ¹¹⁸. Circuitry disruption in rats resulted in regressive behaviours whereby rats demonstrated inability to maintain the new strategy regressing to the previous strategy¹¹⁸.

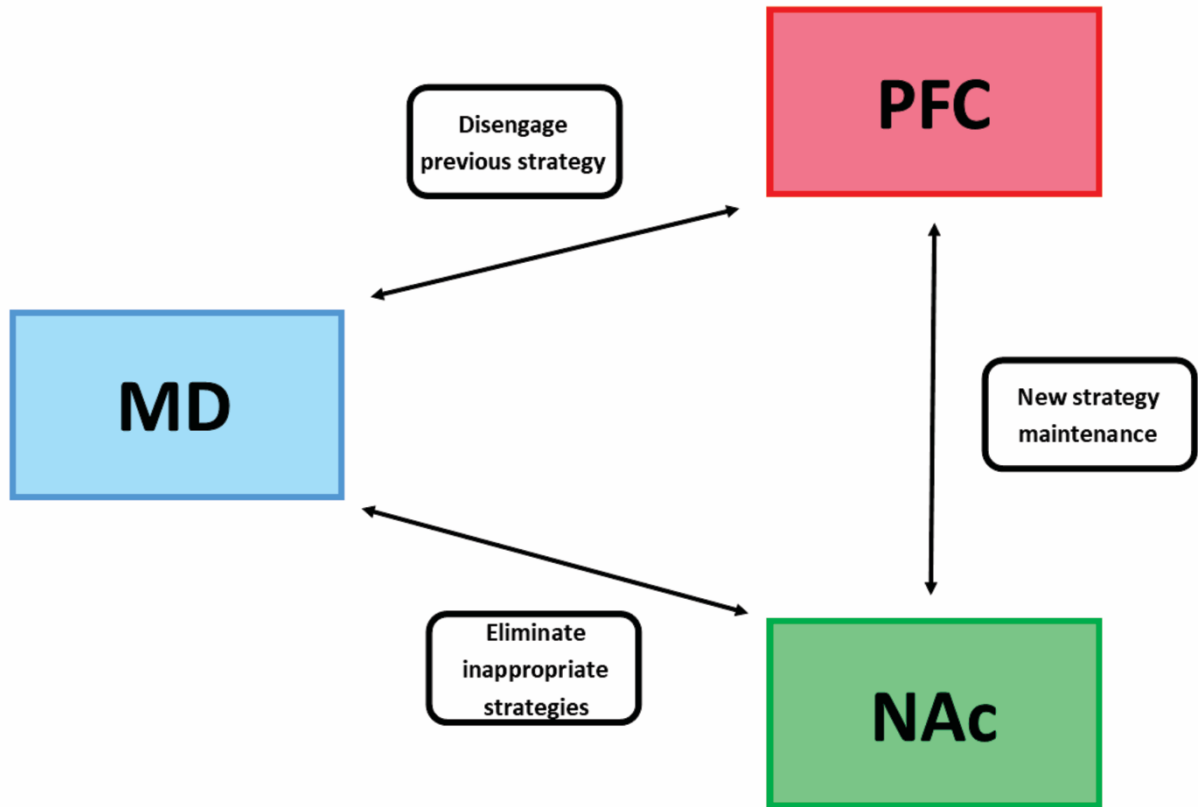


Figure 1.2: Neural circuitry mediating specific components of behavioural flexibility. The prefrontal cortex (PFC), mediodorsal thalamus (MD) and nucleus accumbens (NAc) are involved in mediating behavioural flexibility through the circuitry connecting these structures. Figure modified from Floresco et al (2006)¹¹⁸.

Selectively damaging a specific component of this well-defined circuitry allows researchers to delineate the role that structure plays in executive function, and how it can be affected following injury such as stroke. Thus, modern rodent tests of behavioural flexibility can provide valuable insight into possible mechanisms of ED that can be further explored in humans.

1.10 Rodent models of ischemic stroke

There is a considerable need to create reliable and accurate models of ischemic stroke in order to delineate its mechanistic properties, pathophysiology, and possible interventions in a controlled environment ¹¹⁹. To accomplish this, rats are often employed largely due to their similarities with humans in terms of their cerebrovasculature ¹²⁰. Furthermore, rats are a relatively less costly model that can be easily manipulated to create highly reproducible strokes with predictable post-stroke behavioural outcomes. ¹²¹.

There are a wide variety of ischemic stroke models produced in rats, each with their own benefits and disadvantages. While there are several models of hemorrhagic stroke including decapitation and cardiac arrest, among others, these models produce whole-brain ischemia and are thus unable to be used to investigate the effects of ischemic stroke targeting specific areas of the brain ^{122,123}. Other models, however, allow for focal ischemia to be produced in the brain. For example, the most commonly used focal method is the middle cerebral artery occlusion (MCAO) model ¹²⁴. While this can be accomplished through a craniectomy with surgical occlusion of the vessel, this is extremely invasive, and so it is more commonly accomplished using an intraluminal suture ^{119,125}. In this method, an intraluminal suture is inserted and used to obstruct blood flow within the middle cerebral artery to produce ischemia ¹²⁶. This can be done

permanently or transiently in order to study the effects of reperfusion. While this method is quite commonly used, it carries with it a greater risk for vessel rupture as well as hyperthermia ^{127,128}. Ischemic stroke have also been modelled using emboli either through the injection of thrombi from the animal itself, or artificial thrombi composed of materials such as collagen ¹²⁹ or polyvinylsiloxane ¹³⁰ to produce ischemia ¹¹⁹. As human strokes are most commonly produced by emboli, this model shares a similar origin of ischemia making it highly clinically relevant ¹³¹. This model, however, possess a greater risk of mortality and can produce inconsistent infarcts ¹³². Photothrombosis is a less surgically invasive ischemic stroke model ¹³³. Following the intravenous (IV) injection of photosensitive dye that is sensitive to a specific wavelength of light, a beam of light is exposed to a surface vessel initiating thrombosis within that area to ultimately produce ischemia ^{133,134}. While this model provides many benefits such as low mortality rates and high reproducibility, it produces an infarct with no penumbra, making it less clinically relevant as well as less physiologically representative when used as a model to study pharmacological intervention ^{133,135}. Finally, ischemic stroke is often modelled in animals using injection of the potent vasoconstrictor endothelin-1 (ET-1) to occlude blood flow of target vessels. The greatest vasoconstriction induced by ET-1 occurs at 60 minutes and attenuates to regular flow by the 3-hour mark ¹³⁶. ET-1 can be applied to external vessels or can be injected focally allowing for investigation of the effects of stroke on distinct brain regions. It produces highly reproducible lesions and is associated with lower mortality rates, while not producing physiological or outwardly apparent stress in the animal ¹³⁷⁻¹³⁹. This model would not be useful for studying the mechanisms of neuron repair, as ET-1 can promote axonal sprouting ¹⁴⁰. Additionally, there is a gradual decrease in vasoconstrictive properties over time, so ET-1 lacks precise control over reperfusion time ¹³⁷. While no animal model can fully recapitulate the

complete physiological mechanisms involved in stroke in humans, they each provide a unique, less-invasive approach for researchers to investigate critical processes and interventions that could translate to human studies and stroke treatment.

1.11 Rodent models of WMI

WMI is a key feature of stroke and plays a critical role in post-stroke cognitive impairment. Currently, our understanding on the specific role of WMI with respect to its associative or causal role in post-stroke cognitive impairment is poorly understood. This is due, in part, to a lack of pre-clinical models of focal WMI. Systemic inflammation caused by peripheral injection of inflammatory stimulants or peripheral injury can lead to inflammation within the brain. Systemic inflammation can be induced in animals by cardiac arrest ¹⁴¹, liver failure ¹⁴², acute pancreatitis ¹⁴³ or burns ^{144,145}. Systemic inflammation can also be induced by injections of lipopolysaccharide (LPS), an immunogenic component of the gram negative bacterial cell wall, into the vasculature ^{146,147}. Although these models produce a wide-spread brain inflammation, including within the white matter, a more refined model that selectively targets the white matter tracts is still needed to assess the consequences of white matter inflammation on cognitive decline.

Techniques to induce a more focal WMI within the brain are more limited. One method to induce focal inflammation within the brain is by injection of viruses producing small interfering ribonucleic acid (siRNA). In response to these injections, the brain mounts an inflammatory response to the siRNA as it would to invading viral double-stranded ribonucleic acid (dsRNA) ¹⁴⁸. This technique is still in its infancy and therefore does not have sufficient supportive studies. The most utilized technique of focal WMI induction is via the injection of

LPS. Previous studies have shown that LPS mounts an appropriate inflammatory response within targeted regions of the brain by increasing levels of TNF- α , IL-1, IL-6 and iNOS (inducible nitric oxide synthase) ¹⁴⁹⁻¹⁵². Consequently, this also resulted in the recruitment and activation of astrocytes and microglia and promoted the infiltration of systemic monocytes and neutrophils into the brain ^{149,150,153}. Inflammation and demyelinating damage caused by the LPS injection has also been shown to propagate and spread along white matter connections from a focal initiation. Thus, intracerebral LPS injections have been demonstrated to be a reliable model to study the effects of producing focal inflammation in the brain.

1.12 Rationale, objective, and hypothesis – Aim 1

Clinically, activated microglia persist chronically within the white matter ⁹⁰ and are a strong predictor of cognitive impairment post-stroke ^{84,99}. These findings have also been recapitulated in our lab where unilateral subcortical ischemia in the striatum induced long-lasting bilateral WMI in frontal white matter structures such as the corpus callosum. Additionally, these animals displayed impaired executive function in the form of a regressive behavioural phenotype. This WMI was positively correlated with ED whereby rats with the greatest amount of WMI was the most impaired when assessed behaviourally (unpublished data).

To further investigate the underlying role of WMI in cognitive decline, work in this thesis aimed to assess if WMI and ED could be a consequence of focal stroke in the MD. This region was chosen since it is part of the same circuitry as the dorsal striatum, the site of focal stroke in previous studies. The MD is also a common target of small vessel (lacunar) infarcts ¹⁵⁴, is well-connected to the prefrontal cortex and plays a critical role in executive function ¹⁵⁵. Finally,

clinical studies have shown that stroke targeting the MD impairs the MD, dorsal striatum, PFC circuitry resulting in impairments in executive function ^{156,157}.

We hypothesized that white matter inflammation post-stroke will correlate with impairments in behavioural flexibility. Additionally, we evaluated the outcomes following either unilateral or bilateral stroke. We further hypothesized that rats with bilateral MD stroke will show greater white matter inflammation than animals with a unilateral MD stroke resulting in strong levels of behavioural inflexibility.

1.13 Rationale, objective, and hypothesis – Aim 2

To date, research in our laboratory has demonstrated a correlative link between WMI and behavioural inflexibility, a measure of ED. It is unclear whether the inflammation within the white matter tracts causes, or is simply associated with, the observed behavioural inflexibility. Therefore, the second of AIM of this thesis was to establish whether selective white matter inflammation induced by LPS injections into the corpus callosum (CC) result in impairments in behavioural flexibility. We hypothesize that white matter inflammation is sufficient to cause impairments in behavioural flexibility. Lipopolysaccharide, or LPS, is a cell wall component of gram-negative bacteria, and it has been well-established using both systemic and focal injections as a model of producing neuroinflammation ^{146,147,149–153}. Additionally, LPS injections have been shown to produce significant inflammation in the white matter ^{149–153}. In comparison to WMI seen in animal models of stroke that could have a number of confounding factors aside from inflammation contributing to cognitive impairment, this would produce a pure model of WMI that will allow us to determine whether white matter inflammation is causative of cognitive

impairment. The CC was chosen as the site of LPS injection because it has been found that animals with the most inflammation in anterior white matter structures such as the CC, they were the most impaired in the set-shifting task, giving us an effective area to target to see if WMI can cause ED (unpublished data).

Section 2: METHODS

2.1 Animals

All animal use and procedures were in accordance with the Canadian Council on Animal Care and approved by the Animal Care Committee at Western University (Protocol 2014-016). Sixty 6-month male homozygous wildtype (WT) Fischer 344 rats were used in total for experiments in Aims 1 and 2. Rats were bred and aged, housed in pairs within the Animal Care and Veterinary Services at Western University and kept on a 12:12 hour light/dark cycle alternating at 1 AM/PM. Behavioural testing always occurred during the dark cycle.

2.2 Endothelin-1 focal ischemia model

Focal cerebral ischemia was accomplished using an injection of the potent vasoconstrictor endothelin-1 (ET-1) into the subcortical mediodorsal thalamus (MD). This stroke model has been shown to produce small lacunar infarcts that are commonly observed clinically in precise targets that are highly reproducible^{137,138}. When injected, ET-1 induces focal ischemia of the surrounding vessels with the greatest vasoconstriction induced at 60 minutes and attenuates to regular flow by the 3-hour mark¹³⁶. Prior to surgery, rats were injected subcutaneously with 0.03 mg/kg buprenorphine diluted in 0.9% sterile saline. ET-1 was dissolved in sterile saline to a concentration of 10 pmol per 1 μ L. ET-1 was stored at -80 °C in 10 μ L aliquots. Rats were chosen at random to receive either a unilateral injection of ET-1 into the right MD or a bilateral injection of ET-1 into the left and right MD, (AP -2.9, ML \pm 0.7, DV -5.3) using a 32-gauge Hamilton syringe (Hamilton Company, Reno, NV, USA, n=10 for all groups, 1 μ L volume per injection). Following injection, rats were given an intramuscular injection with 0.03 mL of Baytril (Bayer Inc., Toronto, ON, Canada). Controls underwent an identical surgical procedure with the exception of receiving either a unilateral injection of 1 μ L saline into the right MD, or a

bilateral injection of 1 μL saline into both the left and right MD. A 15% post-surgery (24-hours) mortality rate and a 6% mortality rate during the 28-day post-surgery period before euthanasia was observed.

2.3 Lipopolysaccharide injections

Lipopolysaccharide (LPS) is a component of the cell wall of gram-negative bacteria, and produces neuroinflammation following systemic or focal injections^{146,147,149,150,153,158}. Prior to surgery, rats were injected subcutaneously with 0.03 mg/kg buprenorphine diluted in 0.9% sterile saline. LPS was dissolved in sterile saline to a final concentration of 5 $\mu\text{g}/1 \mu\text{L}$. LPS was stored at $-80 \text{ }^\circ\text{C}$ in 10 μL aliquots. Rats were chosen at random to receive either a bilateral injection of LPS into the left and right CC (AP +1.2, ML \pm 1.8, DV -3.0) or control injections of saline using a 32-gauge Hamilton syringe (Hamilton Company, Reno, NV, USA, n=10 for all groups; 2 μL volume per injection). Following injection, rats were given an intramuscular injection with 0.03 mL of Baytril (Bayer Inc., Toronto, ON, Canada). A 9% post-surgery (24-hours) mortality rate and 4% mortality rate during the 28-day post-surgery period before euthanasia was observed.

2.4 Behavioural Testing

2.4.1 Strategy set-shifting

After a 21-day recovery period following surgery, rats were assessed using a strategy set-shifting task where rats were required to shift from a visual cue strategy to a location-based response discrimination strategy¹⁵⁹. One rat was omitted from results due to an inability to complete this task.

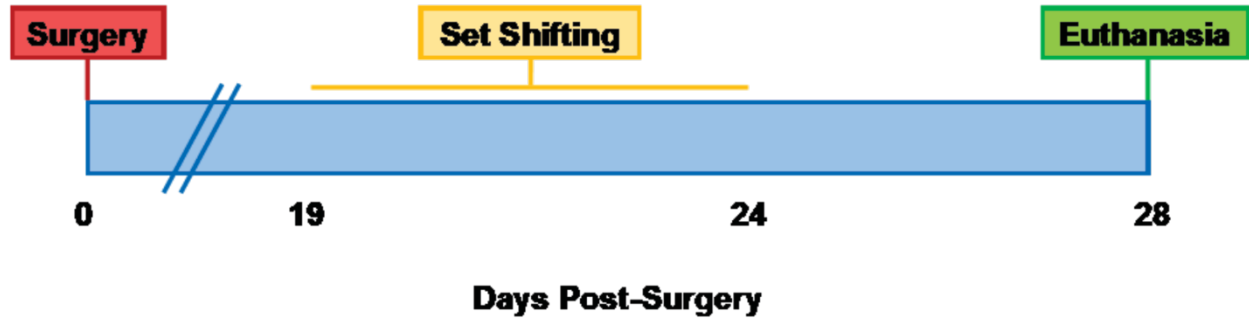


Figure 2.1: Surgical and behavioural timeline for ET-1 study. Surgery was performed (injection of 10 pmol ET-1 in 1 μ L saline, or 1 μ L saline) at approximately six months of age. Rats recovered for 19 days, followed by behavioural testing using an assessment of strategy set-shifting. Rats were euthanized at 28 days post-surgery.

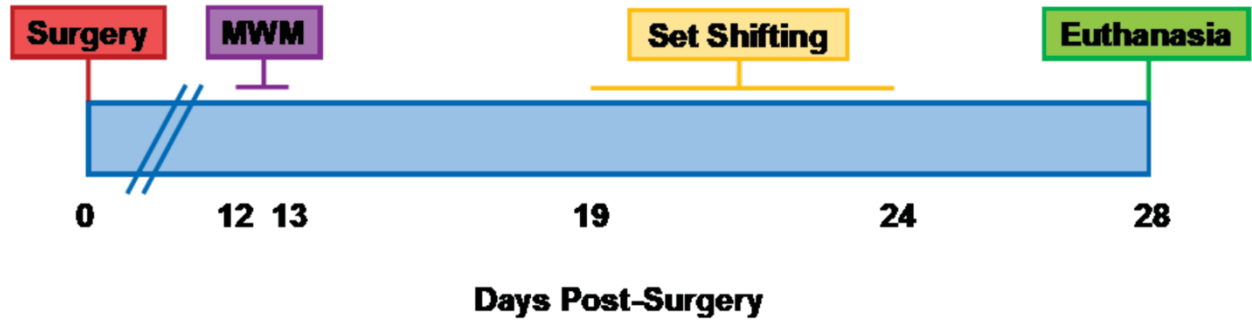


Figure 2.2: Surgical and behavioural timeline for LPS study. Surgery was performed (injection of 10 μg LPS in 2 μL saline, or 2 μL saline) at approximately six months of age. Rats recovered for 12 days, followed by behavioural testing using the Morris water maze (MWM) and strategy set-shifting assessments. Rats were euthanized at 28 days post-surgery.

2.4.1.1 Food restriction

During the pre-testing period, rats were given *ad libitum* access to both food and water. Food restriction was initiated 6 days prior to the testing period. Prior to restriction, rats were weighed, and the pre-restriction weight was recorded. Pair-housed rats were then restricted to a target weight of approximately 85% of their initial weight in order to motivate them to fully participate in the food-motivated testing. Rats were weighed every second day for the remainder of the testing period. Water continued to be provided freely. For 2 days prior to testing, rats were provided with approximately ten sucrose pellets each day in order to familiarize them with the food rewards that would be used in testing.

2.4.1.2 Apparatus

Rats were placed in one of two sound-attenuating chambers with retractable levers in front of them on either side of the chamber, each with a stimulus light above them (Figure 5). Rats were tested in the same box for the duration of the experimental period. A food hopper was present in the middle of the two levers to provide food rewards. A house light was located at the back of the chamber. All testing was completed using the program MED-PC (Med Associates, VT, USA). This program allowed for automated control of all components of the experimental procedure. All procedures were recorded using a portable camera mounted to the roof of the chamber (Grand & Toy, Canada). Testing was performed at the same time in the dark cycle daily until completion of all testing.

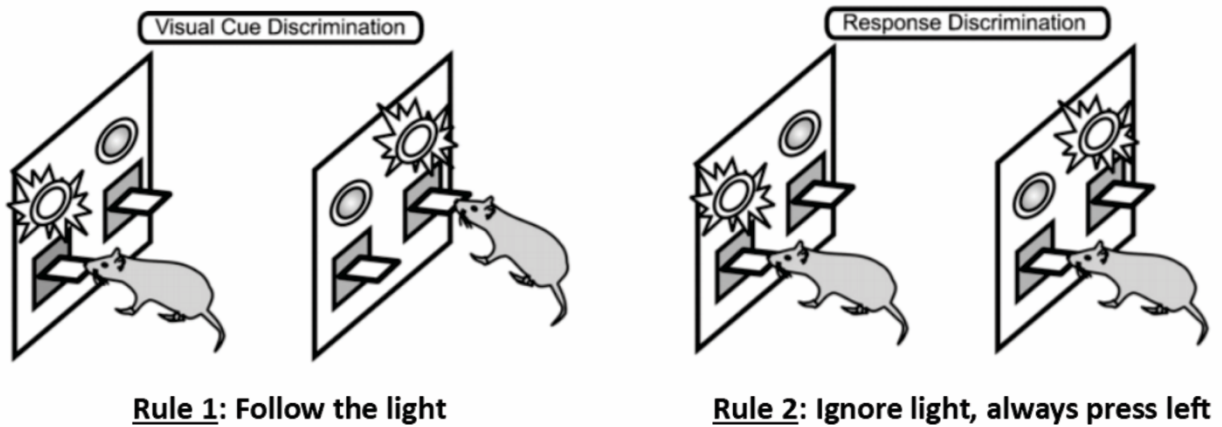


Figure 2.3: Set-shifting behavioural task apparatus and strategies. Animals were initially trained in a strategy where they were required to press the lever that corresponded to an illuminated stimulus light to receive a food reward. They were then required to abandon this strategy to adopt a novel spatial strategy where they were required to only press the lever on one side of the chamber (ie. left lever) to be rewarded. Figure adapted from Floresco et al. (2008)¹⁵⁶.

2.4.1.3 Training

One day prior to the initiation of training, rats were placed in the testing apparatus for 20 minutes to habituate them to their testing surroundings. On the first training session, rats were manually trained to lever press using operant conditioning to form an association between lever pressing and the pellet reward. In this non-automated training task, I had full control over retractable lever movement and pellet dispensing. Successful task completion required the rat to press the left lever 15 times, the right lever 15 times, and finally 15 alternations between the left and right levers.

The following day, rats completed a fully automated training procedure used to ensure they could reliably lever press and had the capability to do so for the entirety of the testing period. Rats began this training session in the dark chamber with both levers retracted. A trial began once the house light illuminated to reveal an extended lever, at which time the rat would have ten seconds to respond by pressing the lever. During these trials, each lever was presented in a counterbalanced manner, with each being presented 50% of the time. If the rat responded correctly, they would receive one 45 mg banana-flavoured sucrose pellet (Dustless precision pellets, Bio-Serv, NJ, USA) from the food hopper immediately following lever pressing. The house light would then remain illuminated for 3 seconds. If the rat failed to respond an omission was recorded and the house light went out immediately and no food reward was received. This training session consisted of 90 trials, with a 20 second inter-trial period. Successful completion consisted of scoring five or fewer omissions throughout the task.

2.4.1.4 Side bias determination

Following successful completion of training, the side bias (left or right) of each rat was determined. At the initiation of the first trial both levers were extended and the rat received a pellet for responding on either lever. Following the inter-trial period, both levers were presented once again and the rat was required to respond on the opposite lever to receive an award. Seven lever alternation trial pairs were completed in this task. If a rat pressed one lever at least twice as many as the other, this was said to be the rat's side bias. If this did not occur, the lever that was chosen first in at least 60% of the presentations was chosen.

2.4.1.5 Visual cue discrimination testing

In the visual cue discrimination (VD) task, rats were trained to associate an illuminated stimulus light positioned over one of the levers with receiving a food reward. VD testing took place 24-hours following completion of side bias determination. At the beginning of each of the 100 trials, the house light was illuminated for three seconds, followed by extension of both levers and illumination of the stimulus light above one of the levers. In order to receive a food reward, the rat was required to press the lever corresponding to the illuminated stimulus light within the 10 second trial period, and the house light would remain on for an additional 3 seconds. If the rat selected the lever without an illuminated stimulus light, they would receive no reward, the levers would retract, and the house light would turn off immediately. Finally, if the rat failed to respond at all in the 10 second trial, no reward would be provided, the house light would turn off, and the trial would be scored as an omission. During these trials, the stimulus light was illuminated over both levers in a counterbalanced and randomized manner, with each being correct 50% of the time. The rat met the criteria for this task when they responded correctly on 8 consecutive trials

^{116,160}. If this point occurred before the full 100 trials were complete, the rat would remain in the chamber to participate in the remainder of the trials. If the rat failed to meet the required criteria for this task, they were re-tested the following day.

2.4.1.6 Response discrimination set-shift testing

Twenty-four hours following successful completion of VD testing, each rat was provided with 20 VD trials to ensure that the rat had properly internalized the visual cue strategy. Following completion of these trials, rats were assessed as to whether they can shift away from the previously successful visual cue strategy, to a novel response discrimination (RD) spatial strategy. The rat was presented with 120 trials for the response discrimination “set-shift” task. To receive reinforcement, the rat was required to ignore the illuminated stimulus lights and respond by pressing the lever on only the side opposite to their side bias. During these trials, the stimulus light continued to be illuminated over both levers in a counterbalanced and randomized manner, with each illuminated 50% of the time overall. The rat met the criteria for this task when they responded correctly on 8 consecutive trials ^{116,160}. If this point occurred before the full 120 trials were complete, the rat would remain in the chamber to participate in the remainder of the trials. If the rat failed the meet the required criteria for this task, they were re-tested the following day.

2.4.1.7 Response discrimination reinforcement

Twenty-four hours following successful completion of RD testing, each rat was provided with an additional 120 RD trials where they were again required to press the lever on only the side opposite to their side bias. This was completed to ensure that the rat had successfully

internalized the response discrimination strategy. The rat met the criteria for this task when they responded correctly on eight consecutive trials. If this point occurred before the full 120 trials were complete, the rat would remain in the chamber to participate in the remainder of the trials. If the rat failed to meet the required criteria for this task, they were re-tested the following day.

2.4.1.8 Intradimensional reversal testing

Twenty-four hours following successful completion of the additional RD testing day, each rat was given 20 RD trials to ensure that the rat had successfully internalized the location-based strategy. Following completion of these trials, each rat was assessed as to whether they could perform an intradimensional “shift”, where they must learn to press the lever consistent with their side bias, and thus opposite to the side in which they were trained during the RD trials to receive a reward. The rat met the criteria for this task when they responded correctly on eight consecutive trials. If this point was never reached, the rat was said to be unsuccessful in this reversal testing, however, no further testing took place for any rats.

2.4.1.9 Error analysis

While the ability to set-shift can provide important information, the true value of this task in examining executive function comes in the evaluation of individual error types involving the acquisition and maintenance of strategy use¹⁵⁹. There were three types of errors examined during the response discrimination aspect of the task. Perseverative errors involve an inability to shift away from the previous learned strategy. A perseverative error occurred when a rat continued to follow the light when the new spatial strategy was correct. Alternatively, regressive

errors occurred when a rat acquired the new spatial strategy, but then failed to maintain it reverting back to the original visual cue strategy. Finally, never-reinforced errors (NRE) occurred when a rat made a choice that was inconsistent with both strategies. For example, if the light was illuminated over the left lever, and the rat pressed the right lever, it would be considered an NRE. These errors are associated with exploration of new strategies.

2.4.2 Morris water maze

A modified version of the Morris water maze (MWM) training schedule was enlisted to assess spatial learning and memory in the rats used in the LPS experiment ¹⁶¹. Since the MWM is a hippocampal-dependent task, we did not expect to see any memory differences between the two groups, so this task was enlisted to serve as a control to ensure that memory was intact in both the control and experimental groups prior to testing executive functioning.

2.4.2.1 Apparatus

Testing involved rats being placed in a water tank (144 cm diameter) filled with water dyed with black non-toxic acrylic paint in order to eliminate visibility of the platform structure below the water. The water was kept at room temperature. The target platform (12 cm diameter) was placed in the tank and submerged below 3 cm of water. The “platform region” was designated as the area within 7.5 cm diameter from the edge of the platform. The tank was surrounded with black panels fixed with three large symbols for the rats to use in spatial navigation. This was done to prevent visibility of the room to ensure that the only external cues

the rats were using to navigate were the symbols provided. The room was kept dimly lit throughout the duration of testing.

2.4.2.2 Learning trials

The first day of the MWM task consisted of six learning trials where the rat was required to use spatial cues in their environment in order to navigate to a platform hidden under 3 cm of water. This platform remained in a consistent location for the duration of all trials. Three large distal cues were placed around the pool to be used in the rat's spatial navigation.

At the beginning of each trial, the rat was placed in the pool facing backwards and allowed to search for the platform location for up to 90 seconds. If they didn't successfully locate the platform, they were guided to it by the experimenter. The rat was then left on the platform for 30 seconds following each trial in order to give time for the rats to spatially map the cues around them to use to locate the platform. If the rat left the platform at any point before this 30 second period was complete, they were gently guided back to the platform and were left there until they remained on the platform for a full 30 seconds. This procedure continued until each rat had participated in six learning trials. Swimming location and additional parameters were recorded throughout all trials.

2.4.2.3 Retention probe testing

Twenty-four hours following the final trial of learning, the platform was removed from the pool. Each rat underwent a probe trial where memory for the prior platform location was assessed. The three distal cues were placed around the pool in the same location as the learning

trials to be used in the rat's spatial navigation. At the beginning of the probe trial, the rat was placed in the pool facing backwards and allowed to swim freely for the 90 seconds duration of the trial. Swimming location and additional parameters were recorded throughout the trial.

2.4.2.4 Visual cue testing

Following testing, rats were assessed using a visual cue task to ensure that their vision was intact. Any issues detected with vision would suggest that rats would not be able to properly complete the task by navigating using the external spatial cues provided. In the first component of this task, the platform was placed in the middle of the northeast (NE) quadrant of the tank with a salient object on top of it, allowing the rats to quickly locate the platform location. Rats were placed in the southeast (SE) quadrant of the pool facing backwards and allowed to search for the platform and salient object for up to 90 seconds. After the rat located the platform, they were immediately removed from the pool and placed back in the southwest (SW) quadrant of the pool facing backward and were allowed to search for the same platform and object location for up to 90 seconds. After successfully locating the platform, the rat was removed from the pool and allowed a 1-hour inter-trial rest period.

In the second component of visual cue testing, the platform was placed in the center of the northwest (NW) quadrant of the pool with a salient object on top of it. Again, rats were placed in the southeast (SE) quadrant of the pool facing backwards and allowed to search for the platform and salient object for up to 90 seconds. After the rat located the platform, they were immediately removed from the pool and placed back in the southwest (SW) quadrant of the pool facing backward and were allowed to search for the same platform and object location for up to

90 seconds. After successfully locating the platform, the rat was removed from the pool and testing was complete.

2.5 Tissue Collection and Preparation

Following completion of behavioural testing, at 28 days post-surgery rats were euthanized by an intraperitoneal injection of sodium pentobarbital (48 mg/mL, Bimeda-MTC, Cambridge, ON). Rats were then perfused transcardially with 0.01 M phosphate buffered saline (PBS, pH 7.4) for 3 minutes followed by 4% paraformaldehyde (PFA) diluted in PBS for 7 minutes. Brain tissue was extracted and then placed in 4% PFA for 24 hours, and then transferred to a solution of 30% sucrose diluted in double-distilled water (ddH₂O) until used for sectioning. The brain was flash frozen on dry ice, sectioned coronally at 30 µm using a cryostat (CryoStar NX50, Thermo Scientific, MI, USA) and then stored in cryoprotectant at -20 °C until processed.

2.6 Thionin Histochemistry

Thionin histochemistry was used to assess cell loss as a result of stroke injury by staining for cellular nissl substance. Free-floating tissue sections were thoroughly washed in 0.01 M PBS to remove all cryoprotectant. Tissue sections were then mounted on SuperFrost Plus slides (VWR International, PA, USA) using 0.3% gelatin, and then allowed to fully dry over 24 hours. Mounted tissue sections were then rehydrated using decreasing concentrations of ethanol from 100% to 50% followed by ddH₂O. The tissue was then submerged in a solution of 0.5% thionin 4 consecutive times and was then transferred to three ddH₂O washes. The tissue was then

progressively dehydrated from 50% to 100% ethanol followed by clearance with xylene. Finally, slides were mounted using DePex mounting medium (DePex, BDH Chemicals, Poole, UK).

2.7 Immunohistochemistry

Tissue sections were stained either with either OX-6 (OX-6, BD Pharmingen, Mississauga, Canada, 554926) as a marker for major histocompatibility complex II (MHC-II) to assess activated microglia, GFAP (GFAP, Sigma-Aldrich, Oakville, Canada, G3893) to assess reactive astrocytes, or neuronal nuclei (NeuN, Millipore-Sigma, Temecula, CA, USA, MAB377) as a marker for neuronal cell bodies. Free-floating tissue sections were thoroughly washed with 0.01 M PBS in order to remove all remaining cryoprotectant. The tissue was then incubated in 1% hydrogen peroxide for 10 minutes (15 minutes for NeuN). Tissue sections were then incubated at room temperature in horse serum blocking solution (Sigma-Aldrich, Oakville, Canada) for one hour, followed by incubation with primary antibody in blocking solution (OX-6: 1:1000; GFAP: 1:500; NeuN: 1:000) at 4 °C overnight. The following day, tissue sections were washed with 0.01 M PBS and the incubated in biotinylated horse anti-mouse secondary antibody in blocking solution (1:500, Vector Laboratories Inc., Burlingame, CA, USA) for one hour at room temperature. Tissue was then incubated in avidin-biotin complex solution (ABC Peroxidase Staining Kit, Thermo Scientific, Rockford, IL, USA) for one hour at room temperature. Tissue was then developed in a solution of 3-3-diaminobenzene tetrahydrochloride (DAB, Sigma-Aldrich, Oakville, Canada) in hydrogen peroxide. Tissue sections were then mounted on glass slides (VWR VistaVision Microscope Slides, VWR International, Radnor, PA, USA) and allowed to dry overnight. Slides were then dehydrated progressively from 50%

ethanol to 100% ethanol, cleared in xylene and mounted with DePex mounting medium (DePex, BDH Chemicals, Poole, UK).

2.8 Microscopy Imaging and Analysis

Tissue sections were analyzed using a Nikon Eclipse Ni-E upright microscope with a Nikon DS Fi2 colour camera head (NIS Elements Imaging). The researcher was blinded to rat experimental condition to prevent bias during analysis. For OX-6, GFAP, and NeuN analysis, 10x magnification images were used for image analysis. For OX-6 and GFAP, images of four tissue sections per rat per stain were taken to assess OX-6 and GFAP immunoreactivity. ImageJ (National Institutes of Health, Bethesda, MD, USA) was used to determine % coverage of OX-6 and GFAP positive staining in the forceps minor (+ 3.00 from bregma) as well as in three different tissue sections of the CC (+1.92, - 0.48 and - 2.92 from bregma) in order to get a representative depiction of immunoreactivity throughout the brain. For NeuN, images of two tissue sections per rat were taken to assess Neu-N immunoreactivity in terms of cell number in the PFC (+ 3.00 from bregma) as well as the NAc (+ 1.92 from bregma). Sections of interest were identified using a rat brain atlas ¹⁶².

2.9 Statistical Analysis

Statistical analyses were conducted using GraphPad Prism software (GraphPad, La Jolla, CA, USA). All figures were prepared using GraphPad Prism in addition to CorelDraw X7 software (Corel, Ottawa, ON, Canada). Data are presented as mean \pm standard error of the mean (SEM). A statistical significance level of alpha 0.05 was used for all tests. Dependent variables

were analyzed using a two-way analysis of variance (ANOVA) with Bonferroni's post-hoc test, an unpaired t-test or an exposure-response logarithmic regression model with Tukey's post-hoc test.

Section 3: RESULTS

3.1 Behavioural assessments – Aim 1

3.1.1 Raw metrics of initial discrimination learning are not affected following MD stroke

Prior to set-shifting, rats were assessed to see whether they could learn a visual cue discrimination strategy whereby they were required to press a lever that corresponded to an illuminated stimulus light to receive a food reward. A two-way ANOVA determined that the number of trials to reach criterion was not affected by ET-1 injection status ($F(1,36) = 0.5096$, $p = 0.4799$) or by the number of injections given (unilateral vs. bilateral; $F(1,36) = 2.835$, $p = 0.1009$) (Figure 3.1 A). Additionally, rats were tested 24-hours later using 20 reminder visual cue trials to determine whether the rats retained learning this initial visual cue rule. A two-way ANOVA determined that there was no significant effect of ET-1 injection status ($F(1,36) = 0.06723$, $p = 0.7969$) or of number of injections given ($F(1,36) = 0.06723$, $p = 0.7969$) on visual cue strategy retention (Figure 3.1 B).

3.1.2 Raw metrics of set-shifting are not affected following MD stroke

After successfully acquiring the visual cue strategy, rats were assessed to see whether they were capable of abandoning this strategy to adopt a novel spatial strategy while ignoring the previously relevant salient visual cues. This allowed the researcher to assess the effects of MD stroke on set-shifting as a measure of behavioural flexibility. A two-way ANOVA revealed no effect of ET-1 injection status ($F(1,36) = 0.02409$, $p = 0.8775$) or number of injections ($F(1,36) = 1.18$, $p = 0.2845$) on trials to criterion when shifting to the response discrimination strategy (Figure 3.2 A). Additionally, it was determined that there was no significant effect of ET-1 injection status ($F(1,36) = 0.06581$, $p = 0.7990$) or number of injections ($F(1,36) = 2.214$, $p = 0.1455$) in the total number of errors to criterion in this task (Figure 3.2 B).

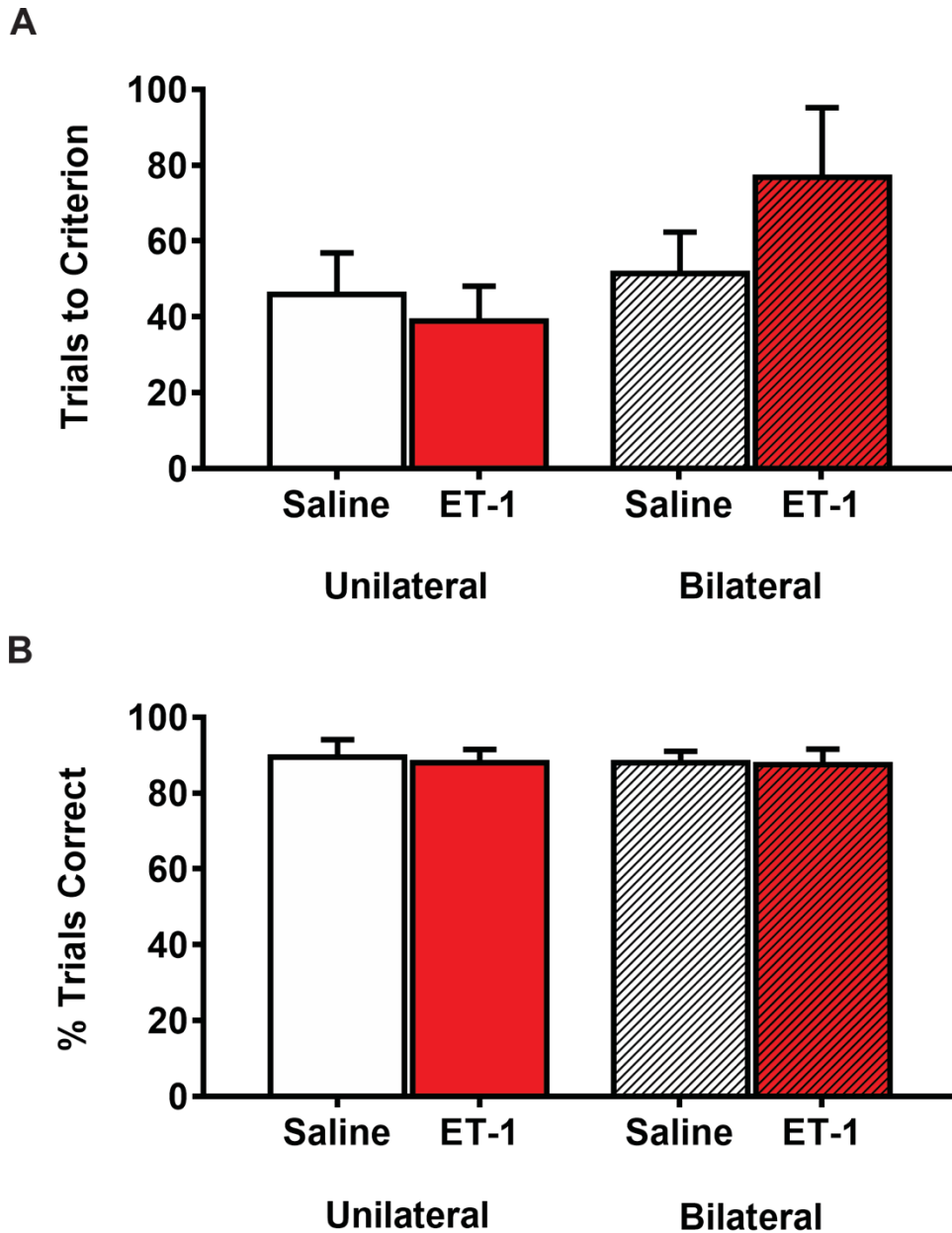


Figure 3.1: Raw metrics of initial discrimination learning are not affected following MD stroke. (A) Number of trials to criterion in the visual cue discrimination task. Criterion was achieved when the animal pressed the correct lever on eight consecutive trials. **(B)** Percent of trials correct when presented with 20 visual cue trials 24-hours following visual cue discrimination testing. Data presented as mean \pm SEM, n=10 per experimental group.

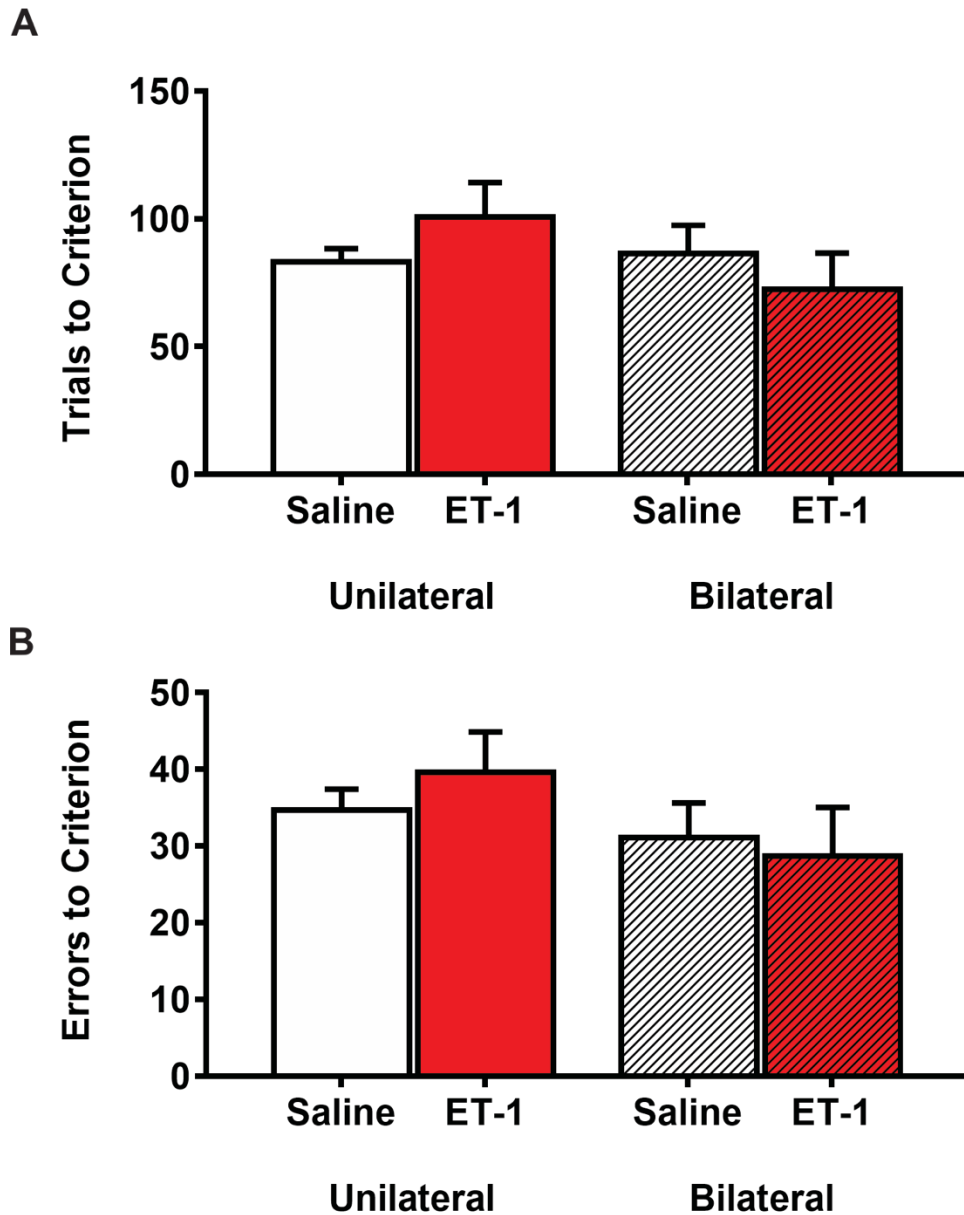


Figure 3.2: Raw metrics of set-shifting are not affected following MD stroke. (A) Number of trials to criterion in the response discrimination task. Criterion was achieved when the animal pressed the correct lever on eight consecutive trials. (B) Numbers of errors before reaching criterion in response discrimination task. Sample size was $n=10$ for all groups. Data presented as mean \pm SEM.

3.1.3 Error profile suggests mild impairment behavioural flexibility following MD stroke

The errors that occurred during RD were further assessed by analyzing perseverative, regressive and never-reinforced errors. Analysis of these error types would provide insight into a rat's ability to abandon a previously successful strategy that no longer provides reward (perseverative errors), how it is able to adopt a new strategy in response to new reward contingencies (regressive errors), and the types of guesses made in strategy exploration (NREs).

In assessing regressive errors, a two-way ANOVA revealed a non-significant effect of number of injection ($F(1,36) = 0.2844$, $p = 0.5971$). Additionally, there was a non-significant effect of ET-1 injection status ($F(1,36) = 2.443$, $p = 0.1268$), however, Bonferroni's post-hoc test identified that unilateral ET-1-injected rats had a significantly greater number of regressive errors (18.6 ± 3.2 errors) than unilateral saline-injected rats (9.4 ± 2.8 errors) ($t(36) = 2.393$, $p = 0.0441$) (Figure 3.3 A). No significant differences were observed when assessing bilateral saline and bilateral ET-1 groups.

While examining perseverative errors, a two-way ANOVA revealed a non-significant relationship between group condition and number of errors where no significant effect was identified for ET-1 injection status ($F(1,36) = 0.3164$, $p = 0.5772$) or number of injections ($F(1,36) = 0.6066$, $p = 0.4411$) (Figure 8B). A similar finding was observed when assessing NREs, where two-way ANOVA revealed no significant effect of ET-1 injection status ($F(1,36) = 0.2221$, $p = 0.6403$) or number of injections ($F(1,36) = 2.345$, $p = 0.1344$) (Figure 3.3 C).

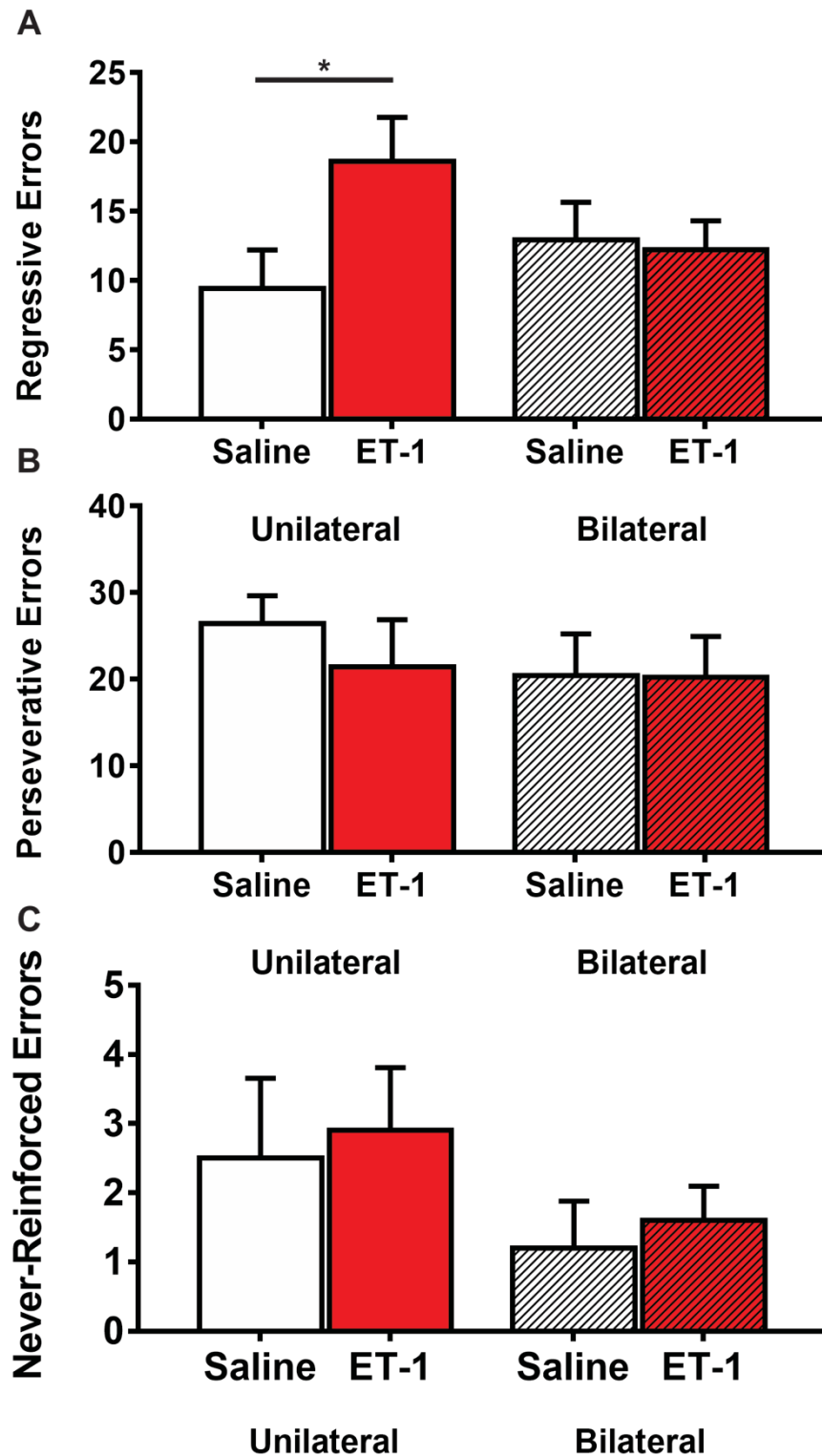


Figure 3.3: Error profile suggests mild impairment in behavioural flexibility following MD stroke. The number of (A) regressive errors, (B) perseverative errors, and (C) never-reinforced errors during response discrimination component of the set-shifting assessment. Data presented as mean \pm SEM. $n=10$ per experimental group. Significance indicated by (*) for $p < 0.05$ (two-way ANOVA).

3.1.4 Modelling logistic regression of incongruent trial error rates following MD stroke

To better represent the relationship between the timing of errors, as well as the timing and efficiency of strategy change, we applied an exposure-response logistic regression model using the mean error rate of each group during each incongruent trial ¹¹⁶. An incongruent trial was defined as a trial in the response discrimination task where the light was illuminated above the incorrect lever for that rat ¹⁵⁹. Thus, to receive a food reward the rat must be following the new location-based strategy. Two measures were taken from the data provided by this regression: (1) the IC50 defined as the number of incongruent trials at which the group is at 50% strategy change, and (2) the hillslope which is defined as the slope of the curve and used to measure group efficiency of strategy change. Using this model, it was determined that the hillslope did not significantly differ between groups ($F(3,224) = 0.9412$, $p = 0.4215$) (Figure 3.4 C). However, a significant difference between groups was identified for the IC50 ($F(3,224) = 0.9412$, $p = 0.0200$), and Tukey post-hoc analysis revealed that bilateral-ET-1 rats had a significantly lower IC50 (27.5 ± 2.9) than bilateral-saline rats (38.9 ± 3.8) ($F(1,36) = 7.207$, $p = 0.0183$) (Figure 3.4 C).

3.2 Histochemistry and immunohistochemistry – Aim 1

3.2.1 Thionin, NeuN and OX-6 analysis of ET-1 injection site(s)

Thionin histochemistry was used to assess cell loss as a result of MD stroke injury by staining for cellular nissl substance. Successful injection location was determined by comparing areas of cell loss to stereotaxic coordinates using a rat brain atlas ¹⁶². Injection location was further validated by assessing neuronal nuclei (NeuN) neuronal loss and OX-6 immunoreactivity at the injection site(s) (Figure 3.5).

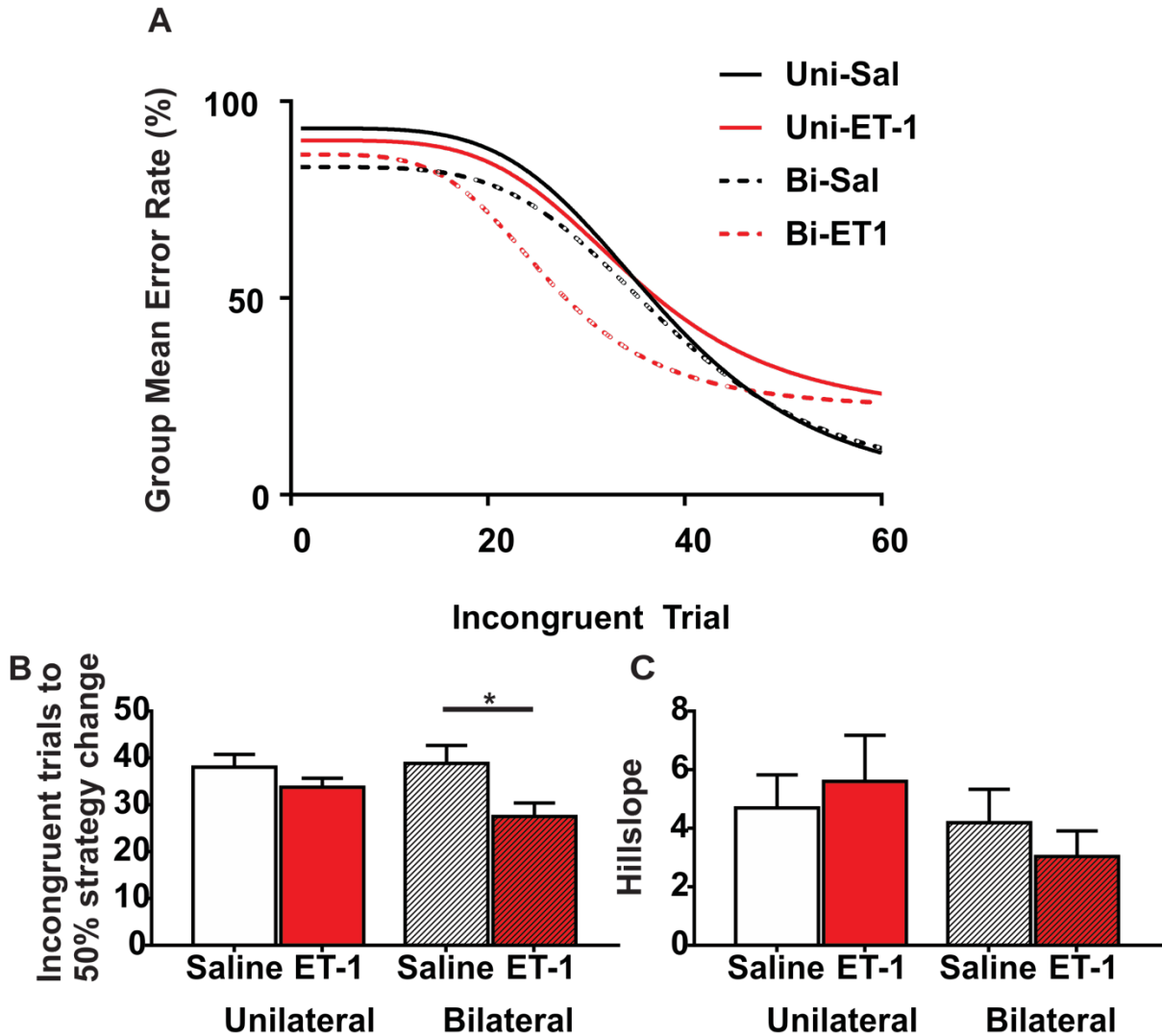


Figure 3.4: Modelling logistic regression of incongruent trial error rates following MD stroke. Data presented as mean \pm SEM, n=10 per experimental group. **(A)** Logistic regression modelling incongruent trial mean error rate. **(B)** Incongruent trials to 50% strategy change demonstrates the number of incongruent trial opportunities taken until 50% of responses demonstrate a change to the new location-based response discrimination strategy. **(C)** Hill slope quantifies the steepness of the curve which is used as a measure of efficiency in switching from a visual cue strategy to a location-based strategy. Significance indicated by (*) for $p < 0.05$ (two-way ANOVA).

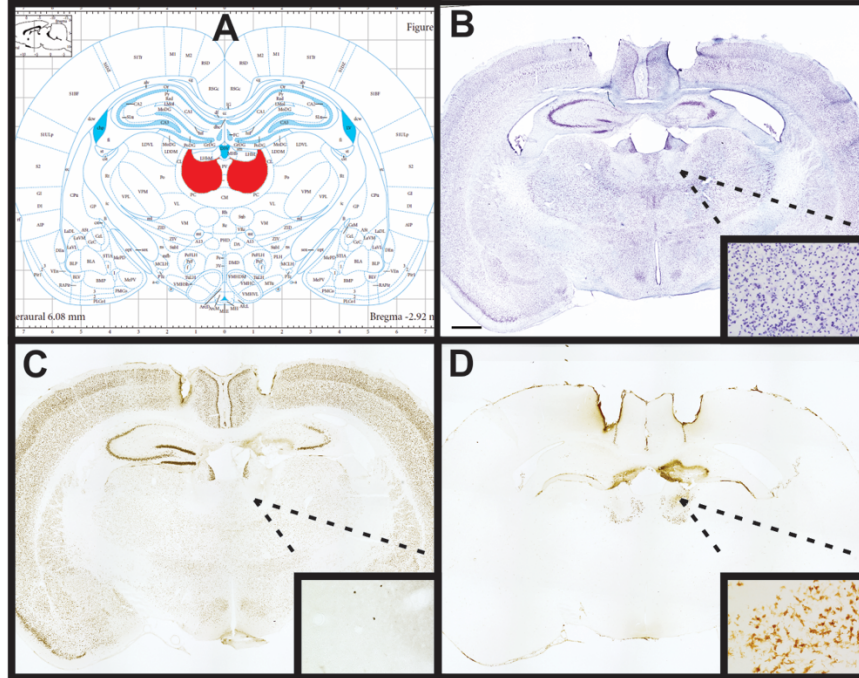


Figure 3.5: Thionin, Neu-N and OX-6 analysis of ET-1 injection site(s). (A) Representative Rat Brain Atlas image of MD injection site(s)¹⁶². Representative 2X images of thionin (B), NeuN (C) and OX-6 (D) stained rat brain tissue used to assess ET-1 injection site(s). Magnified images obtained at 20X magnification. Scale bar is 500 μ m.

3.2.2 No group difference in microgliosis or astrogliosis in the corpus callosum following MD stroke

Microgliosis and astrogliosis were assessed in the CC, a major white matter tract, following injection of unilateral or bilateral ET-1 or saline by analyzing immunoreactivity of the markers OX-6 (activated microglia) and GFAP (astrogliosis). Three separate coronal sections per rat brain per stain were used to assess % coverage of both markers. Values from each section were combined and averaged to give one value of total CC coverage. A two-way ANOVA to assess OX-6 immunoreactivity in the CC identified that was no significant effect of ET-1 injection status ($F(1,36) = 0.5156$, $p = 0.4773$) or number of injections ($F(1,36) = 2.289$, $p = 0.1390$) on % OX-6 coverage (Figure 3.6 I). Moreover, a two-way ANOVA to assess GFAP immunoreactivity in the CC also identified no significant effect of ET-1 injection status ($F(1,36) = 1.198$, $p = 0.2812$) or numbers of injections ($F(1,36) = 0.01551$, $p = 0.9016$) on % GFAP coverage (Figure 3.6 J).

3.2.3 No group difference in microgliosis or astrogliosis in forceps minor following MD stroke

Microgliosis and astrogliosis were additionally assessed in the forceps minor following injection of unilateral or bilateral ET-1 or saline in the MD. One coronal section per rat brain per stain was used to assess % coverage of each marker, and values obtained for both left and right forceps minor were combined and averaged to produce one value of total forceps minor coverage. A two-way ANOVA assessing OX-6 immunoreactivity in the forceps minor revealed no significant effect of ET-1 injection status ($F(1,36) = 0.1931$, $p = 0.6630$) or number of injections ($F(1,36) = 2.052$, $p = 0.1608$) on % OX-6 coverage (Figure 3.7 I). Additionally, a two-

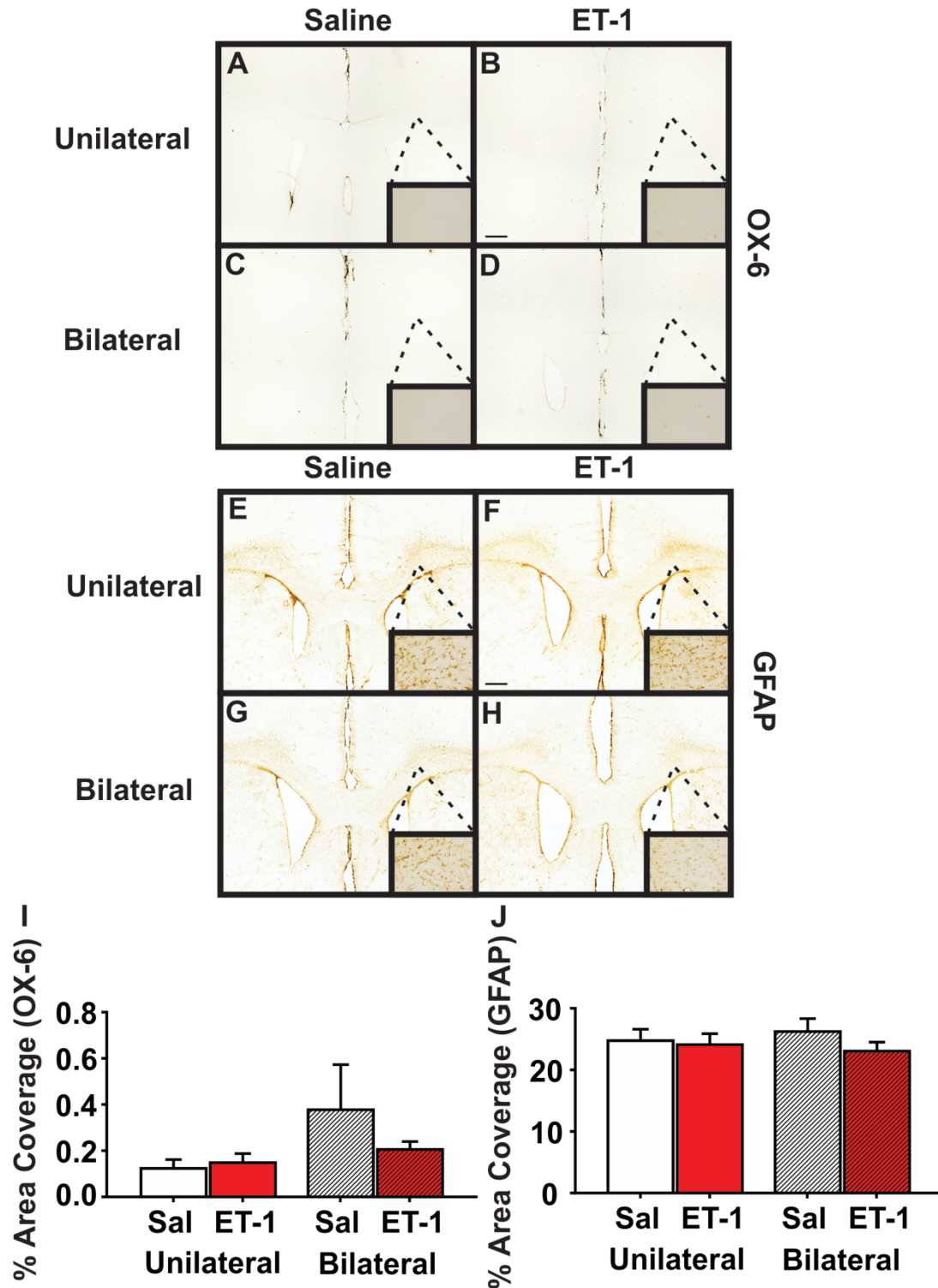


Figure 3.6: No difference between groups in microgliosis or astroglia in the corpus callosum. Representative 2X images of OX-6 (A-D) and GFAP (E-H) stained rat brain tissue. Percent area coverage for OX-6 (I) and GFAP (J) was measured in the corpus callosum of three sections spanning the brain and then averaged. Magnified images obtained at 20X magnification. Sample size was n=10 for all groups. Data presented as mean \pm SEM. Scale bar is 500 μ m.

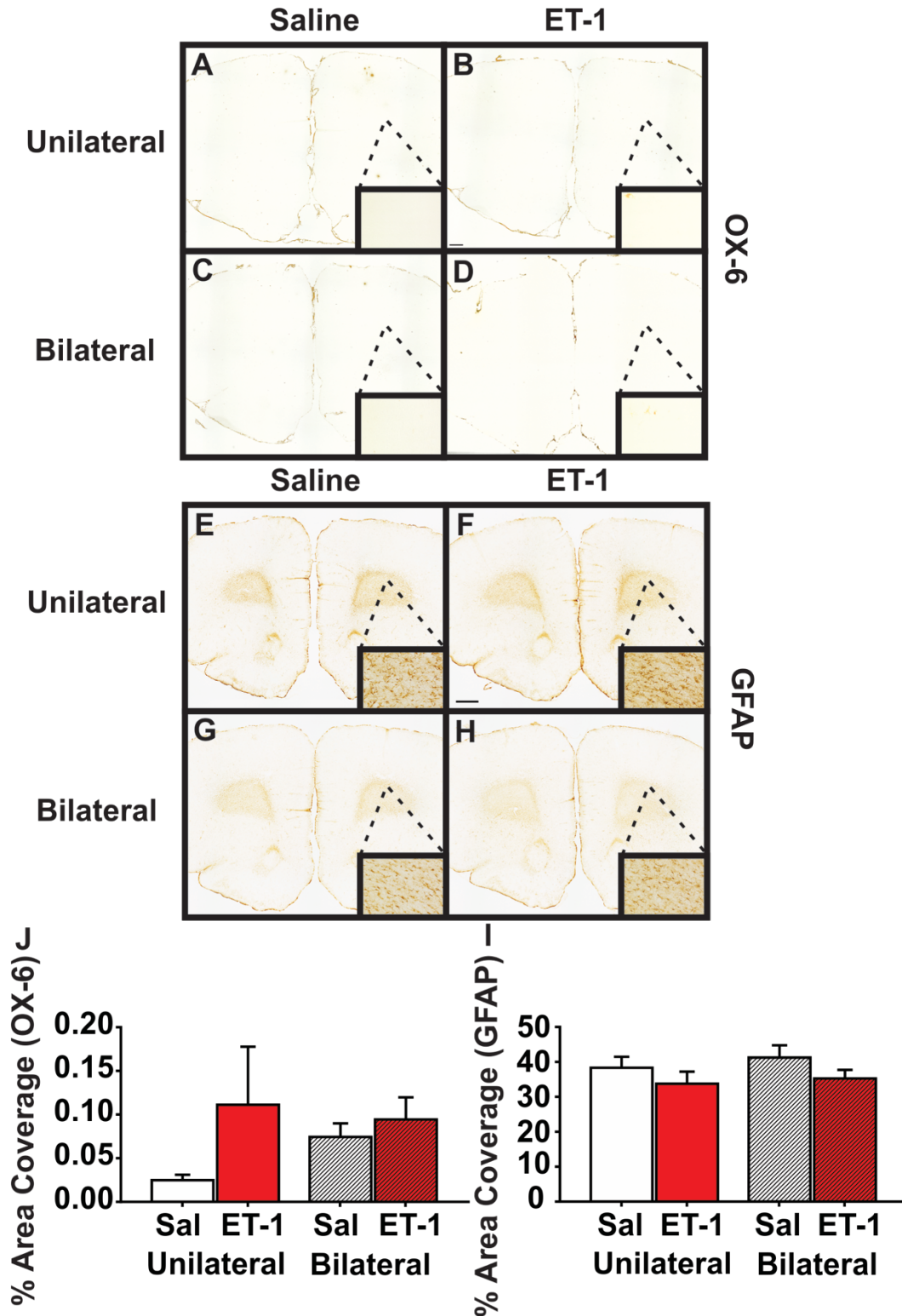


Figure 3.7: No group difference in microgliosis or astrogliosis in the forceps minor following MD stroke. Representative 2X images of OX-6 (A-D) and GFAP (E-H) stained rat brain tissue. Percent area coverage for OX-6 (I) and GFAP (J) was measured in the corpus callosum of three sections spanning the brain and then averaged. Magnified images obtained at 20X magnification. Data presented as mean \pm SEM, n=10 per experimental group. Scale bar is 500 μ m.

way ANOVA assessing GFAP immunoreactivity also revealed no significant effect of ET-1 injection status ($F(1,36) = 0.4978$, $p = 0.4850$) or number of injections ($F(1,36) = 2.881$, $p = 0.0983$) on % GFAP coverage (Figure 3.7 J).

3.2.4 No neuronal loss in PFC or NAc following MD stroke

Neuronal cell bodies were counted in the PFC and NAc following unilateral or bilateral injection of ET-1 or saline by analyzing immunoreactivity of a marker for NeuN. The PFC and NAc were chosen because of their reciprocal white matter connections with the MD and involvement in behavioural flexibility-mediating circuitry. One coronal section per rat brain per area of interest were used to assess the number of NeuN immunoreactive neurons. A two-way ANOVA to assess the number of immunoreactive neurons in the PFC revealed no effect of ET-1 injection status ($F(1,36) = 0.3023$, $p = 0.5858$) or number of injections ($F(1,36) = 0.07112$, $p = 0.7912$) on the number of neurons present (Figure 3.8 I). Furthermore, a second two-way ANOVA to assess immunoreactive cells in the NAc also identified no effect of ET-1 injection status ($F(1,36) = 0.03667$, $p = 0.8492$) or number of injections ($F(1,36) = 0.0008$, $p = 0.9772$) on the number of neurons (Figure 3.8 J).

3.3 Behavioural assessments – Aim 2

3.3.1 Initial discrimination learning not affected but memory for initial strategy slightly impaired following LPS injections

As mentioned previously, prior to set-shifting, rats were assessed to see whether they could learn a visual cue discrimination strategy where they were required to press a lever that

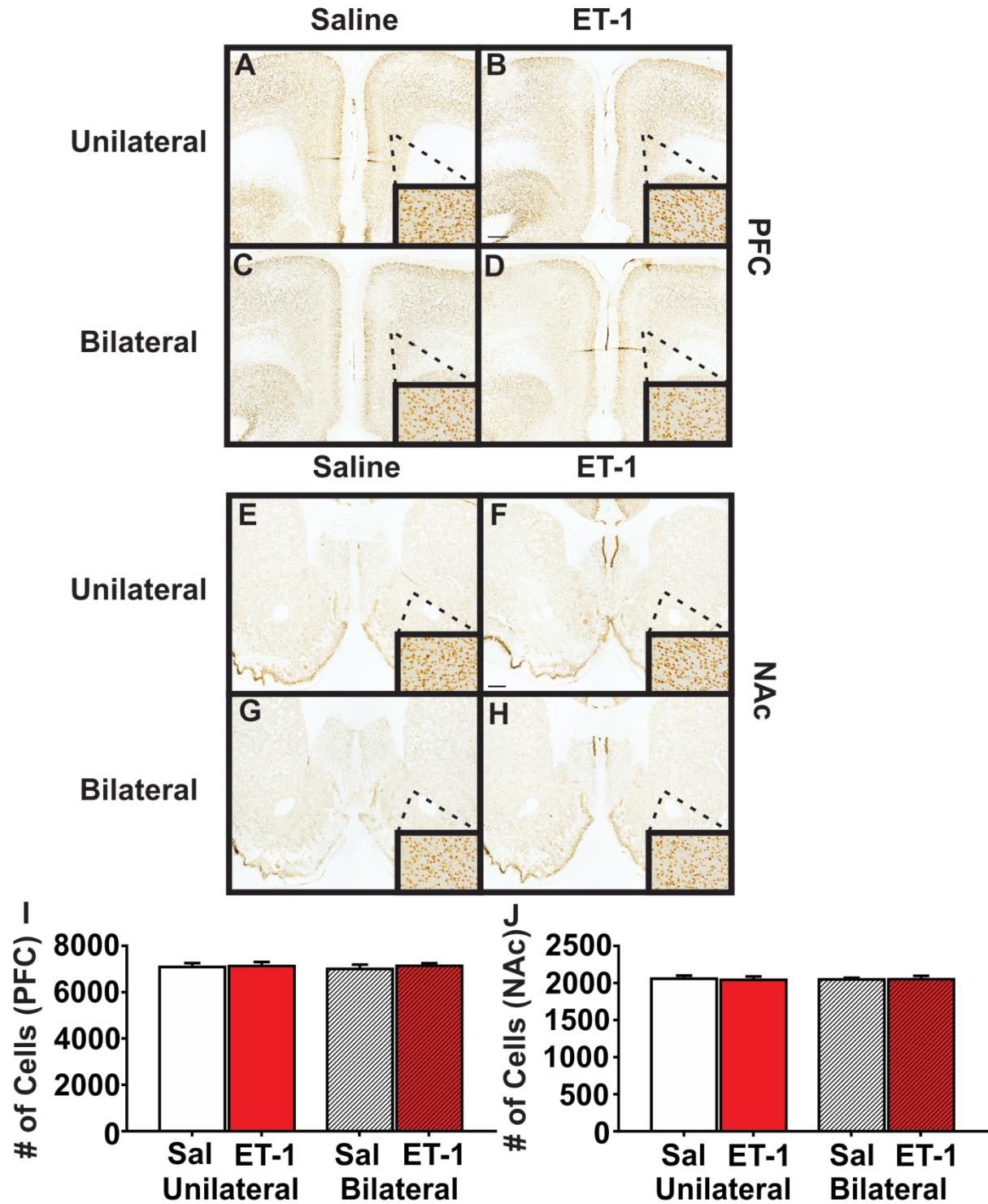


Figure 3.8: No neuronal loss in PFC or Nac following stroke. Representative 2X images of prefrontal cortex (PFC) (A-D) and nucleus accumbens (NAc) (E-H) Neu-N stained rat brain tissue. Number of cells in a 0.61 mm² of the left and right PFC were averaged (I) and the number of cells in a 0.15 mm² area of the left and right Nac were averaged (J). Magnified images obtained at 20X magnification. Sample size was n=10 for all groups. Data presented as mean ± SEM. Scale bar is 500 µm.

corresponded to an illuminated stimulus light in order to receive a food reward. It was found that the number of trials to reach criterion in this task was not significantly different between LPS and saline-injected rats ($t(18) = 1.243$, $p = \mathbf{0.2298}$) (Figure 3.9 A). When rats were tested 24-hours later with 20 visual cue reminder trials for memory of the visual cue strategy, an unpaired t-test determined that there was a significant decrease ($t(18) = 2.233$, $p = \mathbf{0.0385}$) in % trials correct in LPS-injected rats ($89.0\% \pm 2.5\%$) compared to saline-injected rats ($95.5\% \pm 1.6\%$) (Figure 3.9 B).

3.3.2 Raw metrics of set-shifting are not affected following LPS injections

As mentioned previously, following successful completion of the visual cue task, rats were assessed to see whether they could adopt a novel spatial strategy while abandoning the initially rewarding visual cue strategy and ignoring the salient visual cues. This allowed the analysis of LPS injections on set-shifting as a measure of behavioural flexibility. An unpaired t-test revealed no effect of LPS injection on trials to criterion when shifting to the response discrimination strategy ($t(18) = 0.8352$, $p = \mathbf{0.4146}$) (Figure 3.10 A). Additionally, it was determined that there was no significant difference between the two groups in the total number of errors to criterion in this task ($t(18) = 0.0912$, $p = \mathbf{0.3846}$) (Figure 3.10 B).

3.3.3 Error profile suggests no impairment in behavioural flexibility following LPS injections

As described previously, the individual error types from RD were assessed to examine issues associated with novel strategy acquisition (perseverative), strategy maintenance

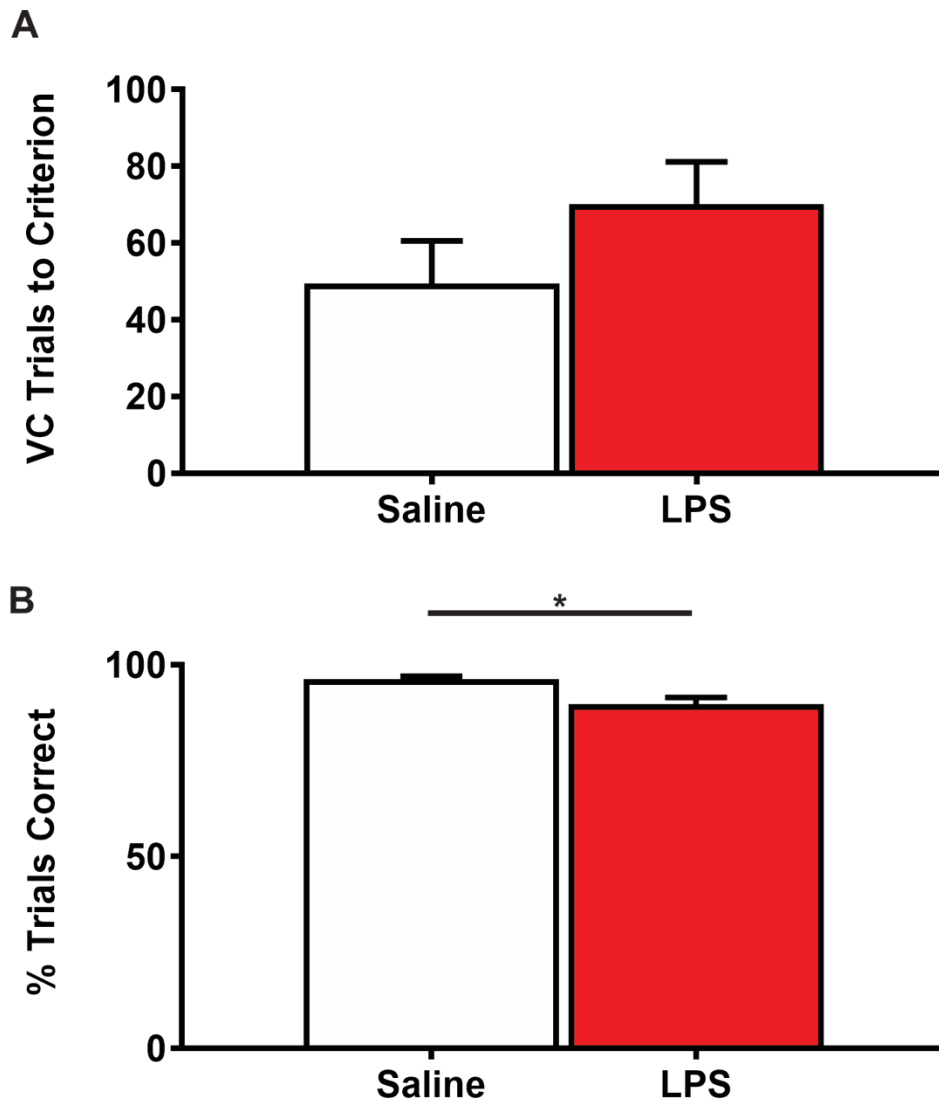


Figure 3.9: Initial discrimination learning not affected but memory for initial strategy slightly impaired following LPS injections. (A) Number of trials to criterion in the visual cue discrimination task. Criterion was achieved when the animal pressed the correct lever on eight consecutive trials. **(B)** Percent of trials correct when presented with 20 visual cue trials 24-hours following visual cue discrimination testing. Data presented as mean \pm SEM, $n=10$ per experimental group. Significance indicated by (*) for $p < 0.05$ (unpaired t-test).

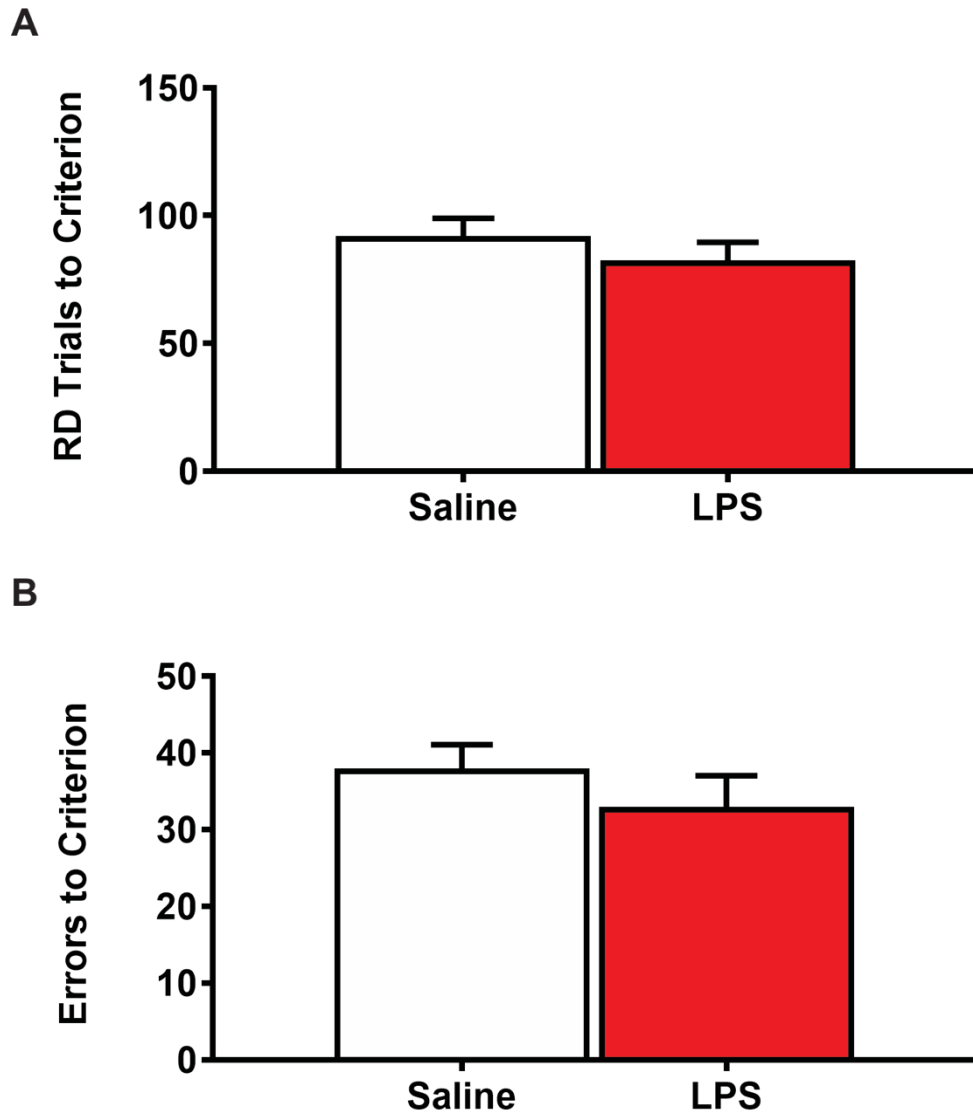


Figure 3.10: Raw metrics of set-shifting are not affected following LPS injections. (A) Number of trials to criterion in the response discrimination task. Criterion was achieved when the animal pressed the correct lever on eight consecutive trials. (B) Numbers of errors before reaching criterion in response discrimination task. Sample size was $n=10$ for both groups. Data presented as mean \pm SEM.

(regressive) and ability to eliminate inappropriate strategies (NRE). Unpaired t-tests determined that there were no significant differences between LPS and saline-injected rats in regressive ($t(18) = 0.7688$, $p = \mathbf{0.4520}$), perseverative ($t(18) = 1.889$, $p = \mathbf{0.0751}$) or never-reinforced errors ($t(18) = 0.9432$, $p = \mathbf{0.3581}$) (Figure 3.11).

3.3.4 Modelling logistic regression of incongruent trial error rates following LPS injections

As described in the aforementioned section, an exposure-response logarithmic regression model was also applied to assess timing and efficiency of strategy change following LPS injections. Using this logarithmic regression it was determined that there was no difference between groups in the IC50 ($t(18) = 0.5503$, $p = \mathbf{0.5889}$) (Figure 3.12 B). However, it was determined that there was a significant difference between groups in hillslope ($t(18) = 2.107$, $p = \mathbf{0.0495}$) where hillslope was significantly steeper for saline-injected rats (7.5 ± 1.4) compared to LPS-injected rats (4.1 ± 0.8) (Figure 3.12 C) indicating that both groups were successfully able to switch to the novel strategy, however, LPS-injected rats switched significantly less-efficiently.

3.3.5 Spatial navigation and memory not affected following LPS injections

Prior to set-shifting, rats were assessed using the MWM to test whether focal injections of LPS resulted in learning and memory impairments. There were no significant differences in latency to platform location between saline and LPS injected rats ($t(18) = 1.316$), $p = \mathbf{0.2047}$) (Figure 3.13). Additionally, when rats were tested for retention of the platform region location

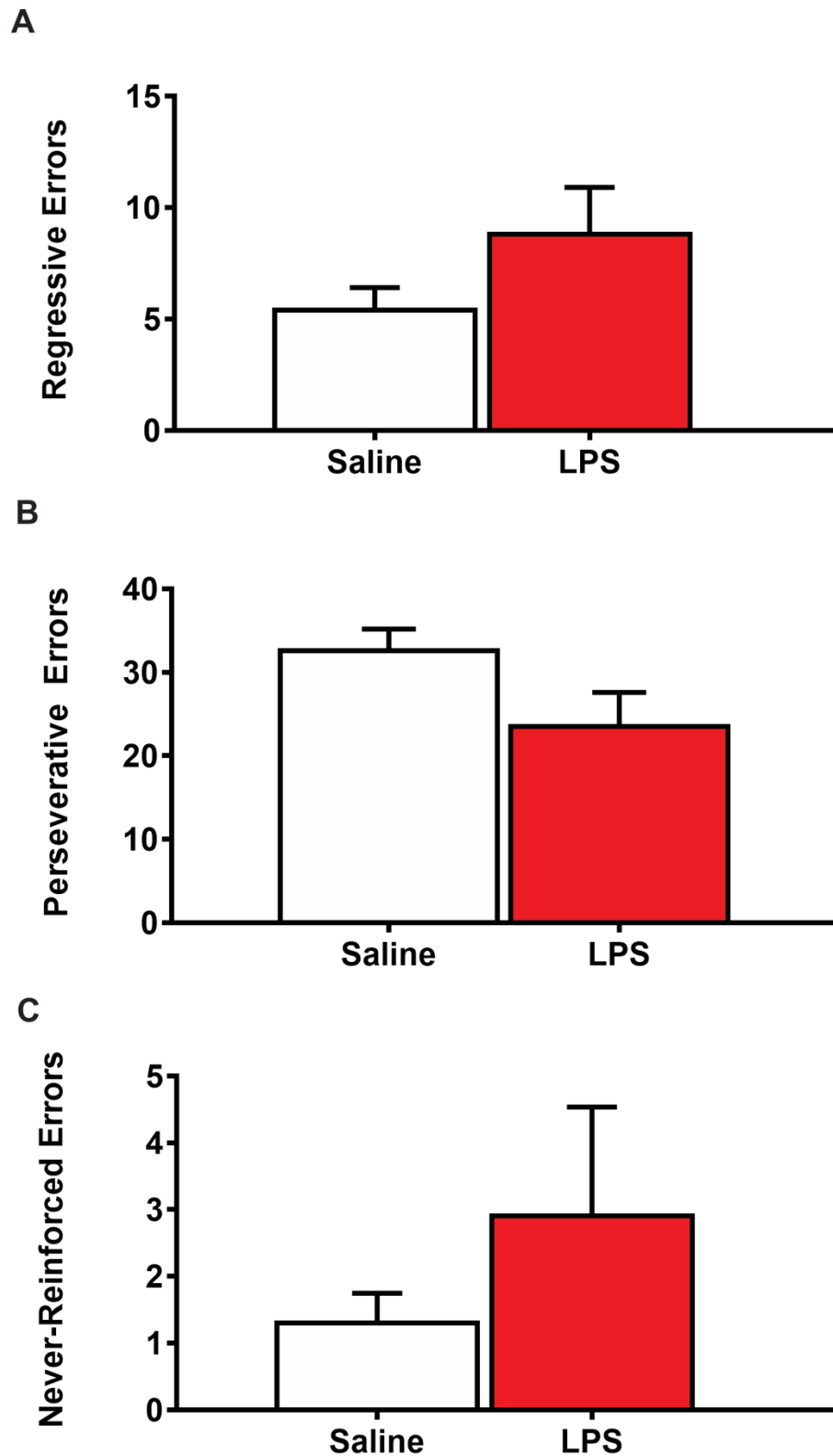


Figure 3.11: Error profile suggests no impairment in behavioural flexibility following LPS injections. The number of (A) regressive errors, (B) perseverative errors, and (C) never-reinforced errors during response discrimination component of the set-shifting assessment. Data presented as mean \pm SEM, n=10 per experimental group.

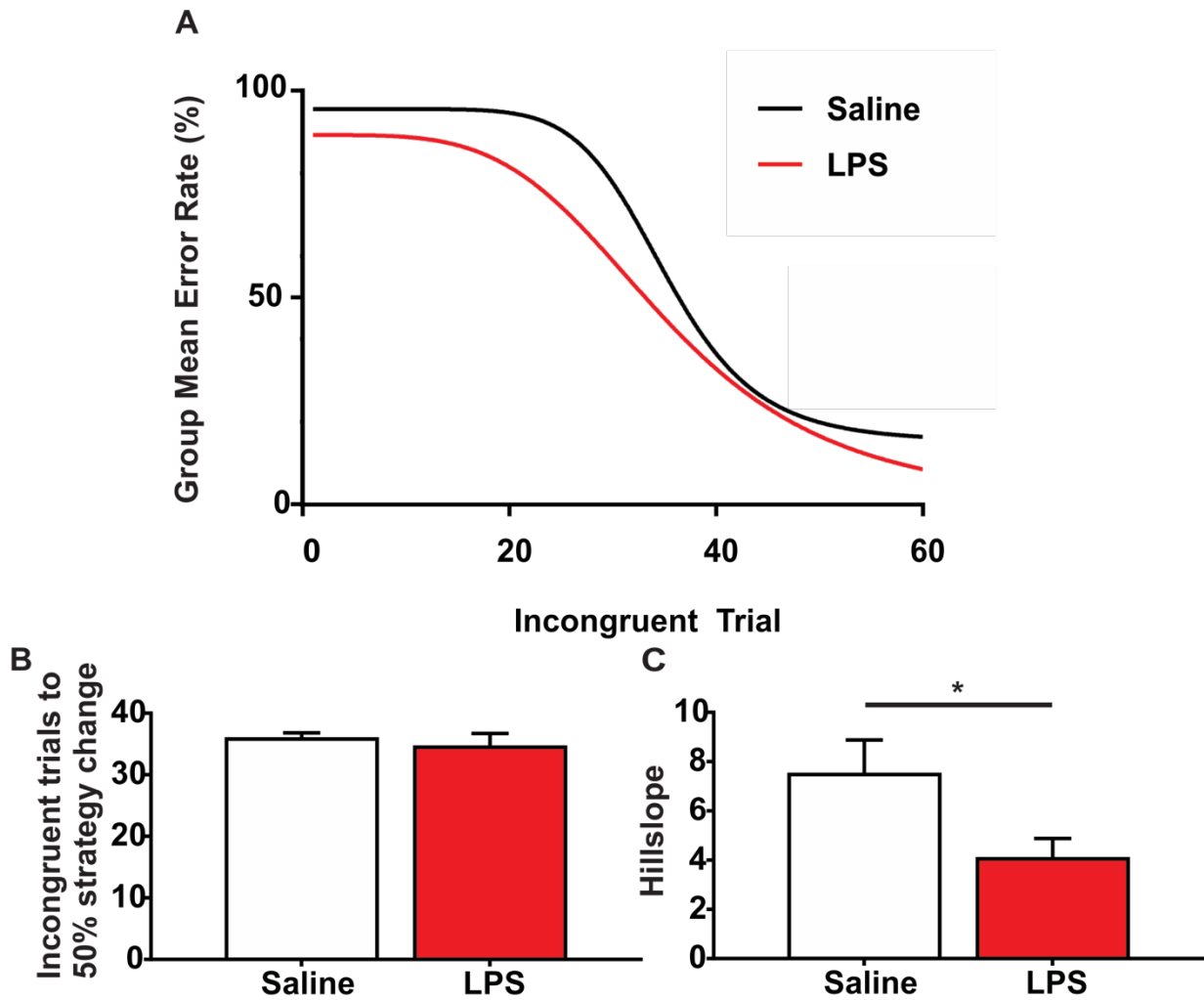


Figure 3.12: Modelling logistic regression of incongruent trial error rates following LPS injections. Data presented as mean \pm SEM, $n=10$ per experimental group. **(A)** Logistic regression modelling incongruent trial mean error rate. **(B)** Incongruent trials to 50% strategy change demonstrates the number of incongruent trial opportunities taken until 50% of responses demonstrate a change to the new location-based response discrimination strategy. **(C)** Curve slope is used as a measure of the hillslope and quantifies the steepness of the curve which is used as a measure of efficiency in switching from a visual cue strategy to a location-based strategy. Significance indicated by (*) for $p < 0.05$ (F-test).

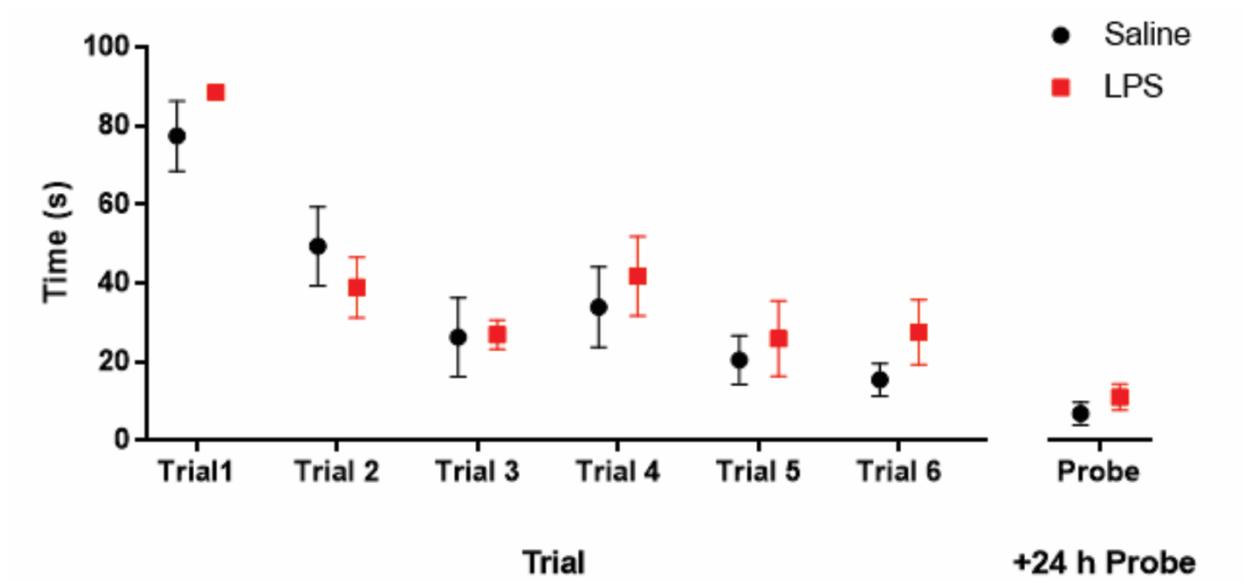


Figure 3.13: Spatial navigation and memory not affected following LPS injections. Average time to the platform in learning trials 1-6 and probe trial 24 hours following training in the Morris water maze. Data is presented as mean \pm SEM, n=10 per experimental group.

24-hours following training there was no significant difference between groups ($t(18) = 0.9447$, $p = 0.3573$) (Figure 3.13).

3.4 Histochemistry and immunohistochemistry – Aim 2

3.4.1 LPS rats had significantly increased microgliosis and astrogliosis in corpus callosum

Microgliosis and astrogliosis were assessed in the CC using three separate coronal sections per rat brain per stain to assess % coverage of both markers. Values from each section were combined and averaged to give one value of total CC coverage. An unpaired t-test to assess OX-6 positive activated microglia in the CC demonstrated a significant increase ($t(17) = 20.78$, $p < 0.0001$) in activated microglia in LPS-injected rats ($57.8\% \pm 2.5\%$) compared to saline-injected rats ($1.6\% \pm 0.4\%$) (Figure 3.14 E). Additionally, an unpaired t-test to assess GFAP immunoreactivity in the CC also identified a significant increase ($t(17) = 2.942$, $p = 0.0091$) in GFAP immunoreactivity in LPS-injected rats ($45.5\% \pm 2.3\%$) compared to saline-injected rats ($32.1\% \pm 4.0\%$) (Figure 3.14 F).

3.4.2 LPS rats had significantly increased microgliosis but not astrogliosis in forceps minor

Microgliosis and astrogliosis were additionally assessed in the forceps minor following bilateral injection of LPS or saline in the MD. One coronal section per rat brain per stain was used to assess % coverage of each marker, and values obtained for both left and right forceps minor were combined and averaged to produce one value of total forceps minor coverage. An unpaired t-test assessing OX-6 immunoreactivity in the forceps minor revealed a significant

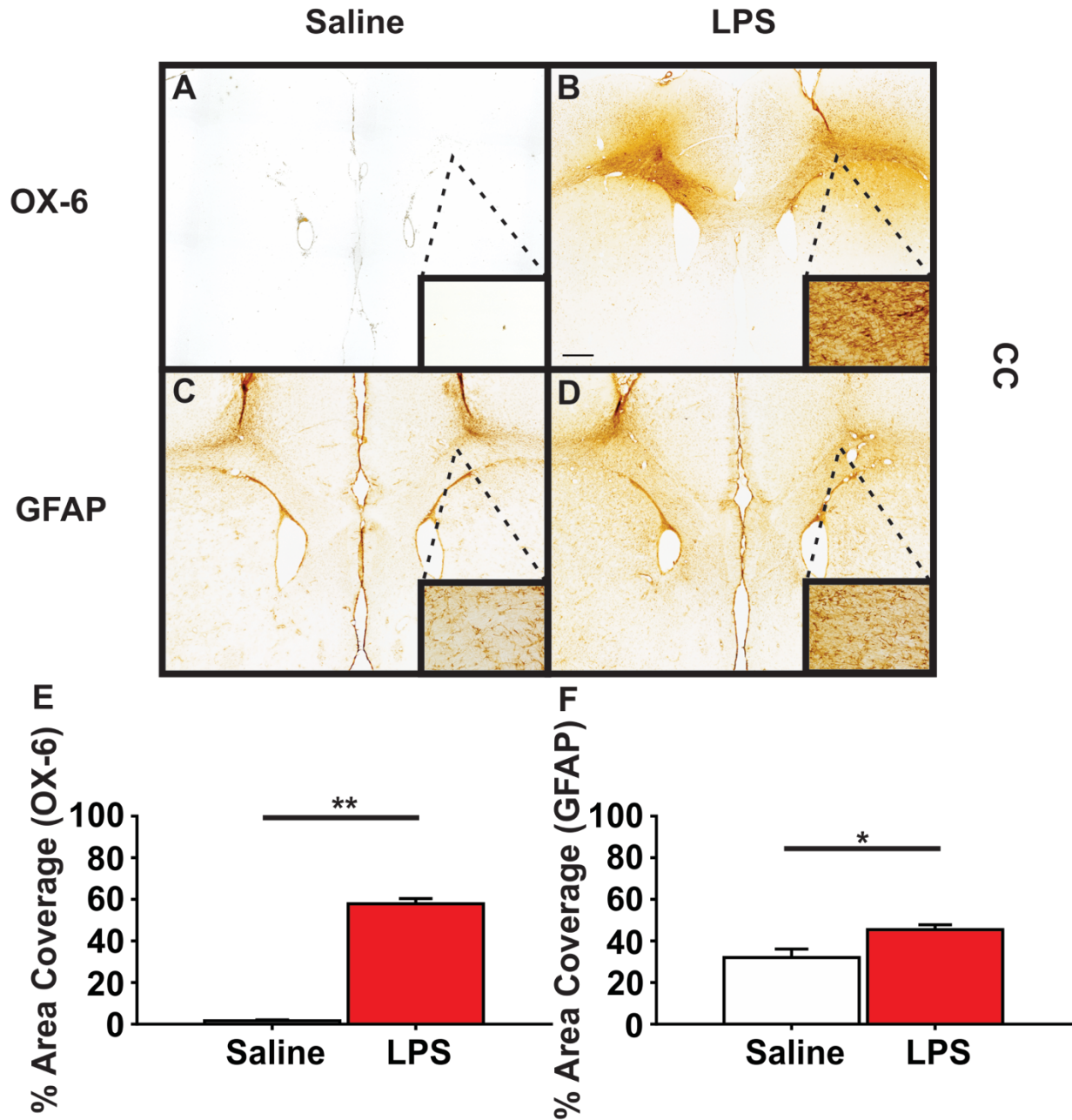


Figure 3.14: LPS animals displayed increased microgliosis and astrogliosis in the corpus callosum. Representative 2X images of OX-6 (A-B) and GFAP (C-D) stained rat brain tissue. Percent area coverage for OX-6 (E) and GFAP (F) was measured in the corpus callosum of three sections spanning the brain and then averaged. Magnified images obtained at 20X magnification. Data presented as mean \pm SEM, $n=10$ per experimental group. Scale bar is 500 μm . Significance indicated by (*) for $p < 0.01$ and (**) for $p < 0.0001$ (unpaired t-test).

increase ($t(17) = 11.89$, $p < \mathbf{0.0001}$) in activated microglia in LPS-injected rats ($70.5\% \pm 5.6\%$) compared to saline-injected rats ($0.3\% \pm 0.1\%$) (Figure 3.15 E). Alternatively, an unpaired t-test assessing GFAP immunoreactivity revealed no significant difference between groups in % forceps minor coverage ($t(18) = 1.868$, $p = \mathbf{0.0791}$) (Figure 3.15 F).

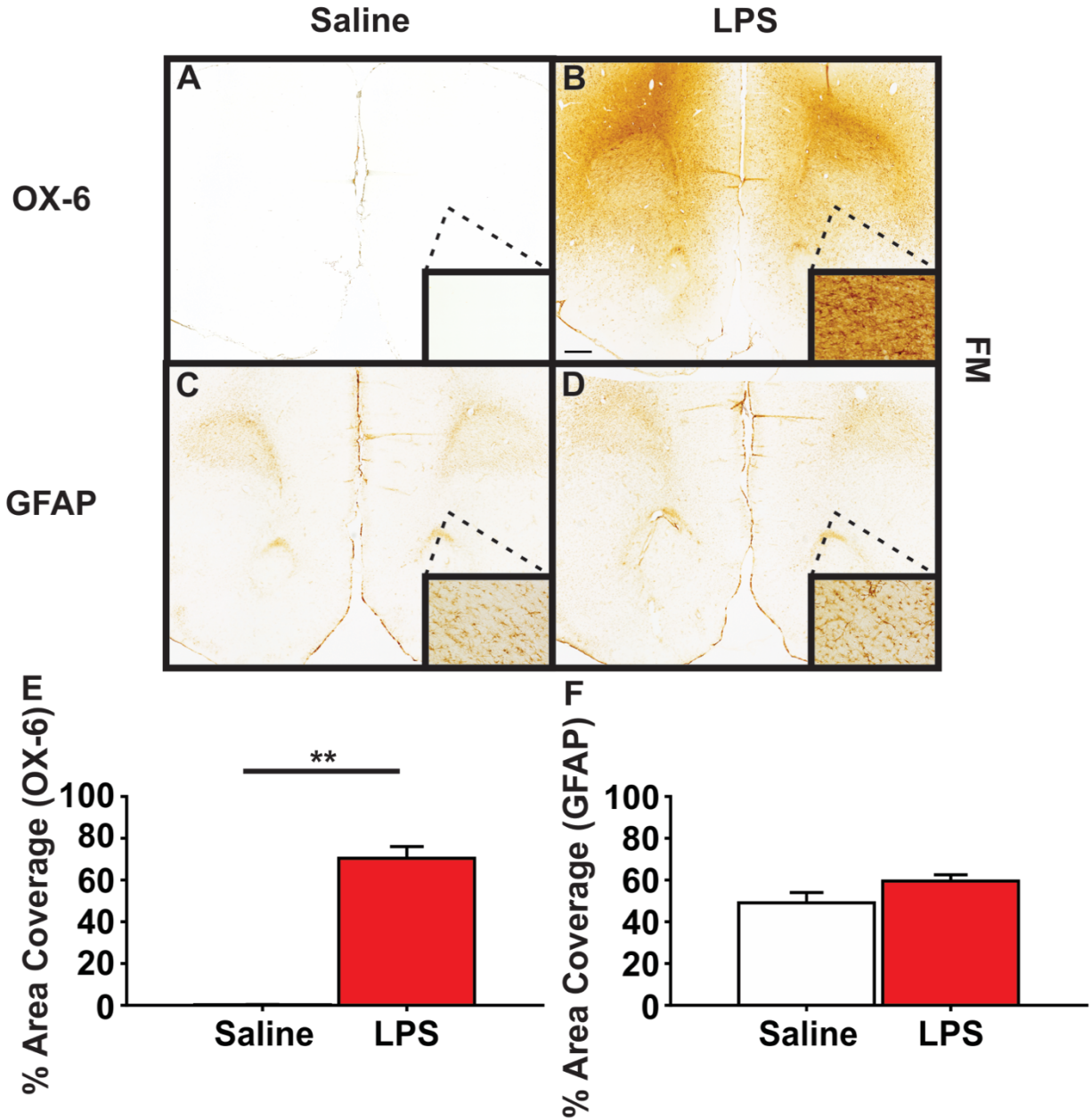


Figure 3.15: LPS rats displayed increased microgliosis but not astrogliosis in the forceps minor. Representative 2X images of OX-6 (A-B) and GFAP (C-D) stained rat brain tissue. Percent area coverage for OX-6 (E) and GFAP (F) was measured in the corpus callosum of three sections spanning the brain and then averaged. Magnified images obtained at 20X magnification. Data presented as mean \pm SEM, $n=10$ per experimental group. Scale bar is 500 μm . Significance indicated by (**) for $p < 0.0001$ (unpaired t-test).

Section 4: DISCUSSION

4.1 Unilateral MD stroke rats displayed mild behavioural inflexibility in the form of a regressive phenotype

The first aim of this study was to determine if focal MD stroke could lead to behavioural inflexibility, a form of ED in rats. Prior to assessing behavioural flexibility, rats were first trained in a visual cue discrimination strategy, followed by testing memory of this strategy the following day. As expected, there were no differences between experimental groups in completing either of these tasks, demonstrating that learning and memory were intact in all groups and behavioural flexibility could be reliably assessed using the set-shifting task.

Initially we had predicted a perseverative phenotype following MD stroke based on the findings from pharmacological inactivation studies where inactivation of the MD led to increased perseverative errors, presumably because of dysfunctional circuitry between the MD and PFC¹¹⁸. This effect was not seen in our study as there were no behavioural changes observed following bilateral stroke, however, we did identify a significant regressive behavioural phenotype following unilateral MD stroke. Interestingly, this is similar to the error profile observed following stroke induced in the dorsal striatum, another subcortical structure that is highly involved in this behavioural flexibility mediated circuitry¹¹⁶.

Previous experimental work outlining the effects of MD lesions and or transient inactivation on executive function has produced conflicting findings, perhaps due to the varying methodologies. For example, one study identified that rats had increased perseveration in a strategy set-shifting t-maze task following bilateral pharmacological inactivation of the MD¹¹⁸. Conversely, in one study assessing the effects on bilateral MD stroke using a digging task of behavioural flexibility, no impairment was identified following MD stroke¹⁶³. Alternatively, an additional study examining the effects of unilateral MD stroke found that in this same task rats

were impaired and required a greater number of trials to reach criterion, however, no perseverative phenotype was identified¹⁶⁴. This ambiguity in experimental findings following MD damage was also reflected in the findings of this study. In our study, it was seen that there was no difference in trials to criterion or total errors during the response discrimination task, however, when the error profile was broken into the three discrete error types, a significant regressive behavioural phenotype was identified. Using this task to assess behavioural flexibility allowed us to identify subtle differences in cognition that may not have been identified using other tests of ED that assess only traditional indices such as ability to complete the task, trials to criterion, total errors, etc. This is one possible explanation for the prior studies that found no effect of MD inactivation on executive function. In addition to assessing the error profile of rats during set-shifting, we also applied an exposure-response logarithmic regression model to the group error rate of the 4 experimental groups. The curve obtained from this analysis allowed us to assess subtle changes that occur in group behaviour by examining the temporal dynamics of strategy change. A significant group effect was identified for the IC50, which is a measure of the number of incongruent trials to 50% strategy change. Bilateral stroke rats reached 50% strategy change sooner than their saline control, suggesting that they were learning to respond to different reward contingencies quicker than controls. However, they did not reach criterion quicker than controls suggesting that while they were able to effectively abandon the unsuccessful visual cue strategy, they could not reliably adopt the novel location-based strategy quicker than controls. It is important to note that most work has focused on pharmacological inactivation or neurotoxic lesion of the MD, with only a few studies investigating the role of the MD post-stroke. A stroke involves several other factors in addition to a MD lesion that need to be considered including recruitment of glia and immune cells, white matter integrity, possible axonal degradation, etc.

Moreover, pharmacological inactivation produces transient effects whereby a structure is inactivated for a short period of time, whereas stroke induces chronic changes that involve different phases of inflammation and healing. The findings of the studies discussed herein, in addition to the findings of this thesis identifying a regressive behavioural phenotype following unilateral MD stroke, all provide evidence for a complexity with respect to the role and function of the MD in mediating executive function. While its circuitry has been well-defined, the practical consequences of MD damage are diverse and further work needs to be completed to delineate the role that it is playing in cognitive impairment.

4.2 MD stroke rats did not display WMI or cell loss in areas of connected circuitry mediating behavioural flexibility

Rat brains were assessed using markers for activated microglia and reactive astrocytes, which are major components of the inflammatory process post-stroke. This was completed in the forceps minor and the CC, two major white matter structures, due to the strong relationship previously observed between WMI and cognitive impairment^{84,94,95,99}. We had predicted that the behavioural phenotype observed in the unilateral MD stroke rats could be explained by increased WMI. In the present study, this was not observed, as there was no significant inflammation generated in either of these structures. The lack of WMI seen in this study was also seen in a similar study performed by Cordova et al.¹⁶³, where an MD stroke was performed on similarly aged (3- to 5-month-old) rats. A later study¹⁶⁴ by the same group found that performing the same stroke in an older (12-month-old) rat could elicit the expected WMI and ED. Additionally, neuron cell number was assessed in two areas with extensive connections with the MD that mediate behavioural flexibility to determine if the regressive behavioural phenotype was due to

neuron loss. It was determined that there was no difference in the number of neurons present in the PFC or NAc between MD stroke and control rats. Therefore, the observed behavioural phenotype cannot be explained by neuron loss. Although the expected inflammation and damage was not seen in our stroke model, similar studies support these results and suggest that age may be largely contributing to the limited pathological response to this type of stroke.

Previous studies have outlined the enhanced susceptibility of the older brain to stroke and some of the underlying cellular mechanisms behind this phenomenon. This includes evidence that older rodents show greater impairment and less recovery from stroke, greater infarct size and neuronal death and greater cytoproliferative activity in astrocytes and macrophages ¹⁶⁵. Furthermore, some studies comparing old and young rats following MCAO showed that sensorimotor function and coordination had recovered in young rats before 14 days post-stroke, but the recovery of the old rats plateaued at 70-85% by 14 days ¹⁶⁶. Other research has shown similar findings and additionally noted a greater decrease in damage and neuroinflammatory markers by 14 days post-stroke in young rats ^{167,168}. Thus, it is possible that the enhanced resilience of young rats to stroke may be protective against persistent white matter inflammation and neurodegeneration.

4.3 LPS-injected rats displayed mild impairment in behavioural flexibility in addition to significant WMI

The second aim of this thesis was to determine whether inducing WMI alone could be sufficient to initiate ED in the rat. Preliminary data from our research group demonstrated that inflammation in frontal white matter structures such as the corpus collosum following a striatal stroke was associated with ED in the form of a regressive behavioural phenotype (unpublished

data). Based on these findings, this study looked at the effects of focal injections of LPS into the CC on behavioural flexibility. We had predicted that inducing WMI in the CC would produce behavioural inflexibility in the form of a regressive behavioural phenotype. As demonstrated by the completion of the visual cue task where there was no difference between groups in the number of trials to reach criterion indicating that LPS-injected rats demonstrated no impairments in learning. While there was a significant difference between groups in memory for the visual cue strategy the following day, LPS-injected rats still performed at a group rate of 89% of trials correct. Additionally, since there was no difference between groups in the MWM memory assessment, we were confident that set-shifting would be an accurate assessment of behavioural flexibility in these rats.

During the response discrimination task, there were no significant differences between groups in the trials to criterion or total errors in completing the task. Additionally, when assessing the complete error profile, there were no difference found between groups regarding the individual error types. Although non-significant, the individual error types in the set-shifting task demonstrated that LPS-injected rats had decreased perseverative errors as well as increased regressive errors. Interestingly, this is the same pattern of errors observed following unilateral striatal stroke ¹¹⁶, and unilateral MD stroke, as observed in the first aim of this thesis. Given the significant inflammation that was induced within the CC, we had expected to see a robust behavioural response, given the strong correlation identified between frontal white matter inflammation and behavioural inflexibility. While a non-significant error profile was observed, ED in the LPS-injected rats was highlighted by the results seen following the application of an exposure-response logarithmic regression model to the group error rate of LPS and control rats. When assessing hillslope, which is a measure of strategy change efficiency, it was found that

control rats had a significantly steeper slope than LPS-injected rats. The point at which 50% strategy change was reached, however, occurred at approximately the same time. These findings indicate that while both groups were able to complete the task and to switch strategies in the same amount of trials, the LPS-injected rats switched strategies with less efficiency. LPS-injected rats abandoned the visual cue strategy sooner as indicated by the earlier decline in the curve, however, it took them longer to identify and maintain the appropriate strategy as indicated by the flatter slope and the corresponding increase in regressive errors. In comparison, saline-injected rats took slightly longer to abandon the initial visual cue strategy, however, once they did they very quickly adopted the novel location-based strategy and maintained this strategy successfully as indicated by the steep slope of the curve. This significant decrease in hillslope was also observed following dorsal striatal stroke in aged rats ¹¹⁶. While the error profile differences were not significant, the findings from this model suggest that there are differences in behavioural flexibility between LPS rats and controls, they may just require more sensitive metrics to tease apart these differences.

When assessing pathological differences between LPS rats and controls, it was evident that focal injection of LPS successfully induced WMI in frontal white matter structures as indicated by a significant increase in microglia in the corpus collosum and forceps minor, as well as significant astrogliosis in the CC. Although WMI has been identified as a strong correlate of behavioural inflexibility, this significant amount of WMI did not produce as robust behavioural phenotype as we had expected. It is possible that the inflammation seen may not be sufficient to cause cognitive impairment within the time-frame utilized in this study. While a 28-day timepoint was sufficient to identify behavioural inflexibility following MD stroke as seen in the first aim of this thesis, WMI alone may take longer to produce an observable behavioural

phenotype. Following a stroke, there is immediate cell death that occurs at the infarct site as well as additional cell damage in the penumbra that surrounds the central core of the infarct. The extent of cell death following the initial stroke depends greatly upon the inflammatory processes that are initiated by this hypoxic event. Alternatively, with focal injection of LPS, the inflammatory process begins with the recruitment of microglia and production of inflammatory cytokines and this may require a longer time period than 28-days to produce cell death or damage on the level that would occur following stroke. Thus, WMI inflammation may require longer periods of time to cause deficits or young may be more resilient to WMI than older rats overall, explaining why a robust behavioural phenotype was not observed following focal LPS injections.

4.4 Caveats and future directions

An important caveat in these studies was only being able to assess pathology 28 days post-stroke. With the extensive behavioural testing that was completed, we had to be sure that the rats recovered fully from their surgeries before testing began to ensure that there were no confounding factors that could affect behaviour in the set-shifting task such as pain or discomfort from wound healing. It would, however, be valuable to include additional rats in the cohort to be sacrificed at different time points beyond the initial 28-day period before sacrifice to get a clearer picture of the pathophysiological changes occurring throughout time.

While a significant regressive behavioural phenotype was observed following unilateral MD stroke, no significant pathological changes were identified in these rats using markers for activated microglia, astrocytosis or neurons. As mentioned previously, due to the young age of these rats, it is possible WMI was transiently present. However, further work must consider the

possibility that damaging effects of the inflammatory process may have compromised white matter integrity that was not visible with the histology completed in this study. Further immunohistological analyses using markers for myelin basic protein (MBP) or degenerating myelin basic protein (dMBP), or histological analyses such as luxol fast blue to assess white matter integrity would provide clarification regarding damage that may have occurred to the white matter following MD stroke. Moreover, it would be valuable to assess possible axonal degeneration, as in a previous study of MD stroke it was identified that while no lasting WMI was observed, axonal degeneration was identified along thalamocortical projections⁹². An additional caveat in this study is that only the effects of bilateral MD stroke and unilateral stroke in the right MD were considered. Since unilateral stroke in the right MD produced behavioural inflexibility but no effects were seen following bilateral MD stroke, it is necessary for future work to consider the effects of unilateral stroke on the left MD only. It is possible that behavioural consequences following left MD stroke could be antagonistic to the behavioural phenotype following right MD stroke resulting in no phenotype being observed following bilateral MD stroke. To our knowledge, no studies have considered the differential effects of unilateral stroke in the right MD compared to the left MD, and these findings would have important consequences for future studies of MD stroke. Moreover, the effects of MD stroke should be further investigated in older rats involving a wide variety of histological analyses to assess WMI, neuronal loss and white matter integrity to observe how these factors can change with age.

Finally, the second aim of this thesis, to our knowledge, was the first investigation of the effects of focally-induced WMI on cognition. These initial findings demonstrating that WMI alone may have subtle effects on behaviour in young rats in addition to the prior clinical and

experimental work relating WMI to cognitive impairment imply that more work is needed to be completed to understand the complex role of WMI. Since the rats used in this study were only 6-months-old, future work should examine the effects of focally-inducing WMI in middle to older age rats to assess how the inflammatory profile and behavioural consequences of inflammation change with age and with the differing levels of basal WMI that exist in these older rats.

Additionally, combining focal LPS injections into the white matter with the induction of subcortical stroke would provide a valuable model to examine how increased levels of WMI can affect stroke pathophysiology and subsequent cognitive impairment. Moreover, the effects of focally-induced WMI should be explored in a chronic manner, either with multiple focal injections of LPS over time or one injection followed by a lengthy survival time period. Finally, while significant correlations have been identified between CC WMI and behavioural inflexibility, there is also diffuse WMI throughout many additional white matter tracts. Thus, it is possible that only inducing inflammation in the CC may be insufficient to produce a robust behavioural phenotype. It would be valuable to determine the effects of focally-inducing inflammation in a variety of white matter tracts in the same model to see how this effects ED. Therefore, allowing WMI to persist for a longer period of time or inducing WMI in a variety of white matter structures may allow for the necessary damaging effects to occur to produce robust behavioural dysfunction.

Section 5: SUMMARY AND CONCLUSIONS

The objective of the first aim of this thesis was to determine whether MD stroke would result in WMI and impairments in behavioural flexibility. It was determined that rats receiving a unilateral MD stroke had a regressive behavioural phenotype, however, this was not paired with inflammation in major white matter structures such as the CC and forceps minor. Additionally, there was no neuronal loss identified in structures connected to the MD that mediate components of behavioural flexibility such as the PFC and NAc. The objective of the second aim of this thesis was to determine whether focally-inducing inflammation in the CC could produce ED in the form of behavioural inflexibility. While these rats did not display a significant behavioural phenotype when assessing traditional error profile measurements, a significant difference was observed in efficiency of strategy change using a logarithmic regression model. Additionally, LPS-injected rats had significant inflammation in the CC and forceps minor.

Although the circuitry of the MD has been well-defined, studies that have targeted the MD up to this point have found inconsistent evidence of the functional outcomes following MD damage or inactivation. Moreover, this body of research is especially lacking in studies investigating the effects of focal MD stroke on cognition. The findings from our MD stroke study provide additional evidence to help delineate the role the MD is playing in cognition. Additionally, while prior work relating WMI to ED has been strictly correlative, our second study provides the first evidence that inducing focal WMI may be sufficient to produce cognitive impairment. While much work still needs to be done to determine the complete mechanism by which WMI contributes to the cognitive dysfunction, this study was a necessary first step in investigating this mechanism and has provided valuable insight to guide future studies of WMI. Both of these studies provide additional evidence for the role that age plays in mediating the effects of stroke and inflammation. In accordance with our findings, a young age may provide

rats with an increased resiliency to the detrimental effects caused by stroke and WMI. Our studies provide valuable models to investigate the effects of MD stroke and WMI as these young rats have limited basal WMI. This, however, provides a need for future studies that investigate ischemic damage and WMI within rats of varying ages to determine age-related changes in behaviour and pathology in these specific models. These future studies will provide valuable insight to the mechanism of WMI, which may ultimately provide potential targets for future therapeutic interventions.

REFERENCES

1. Agence de santé publique du Canada. *Stroke in Canada : highlights from the Canadian Chronic Disease Surveillance System*.
2. Wolf, P. A., Abbott, R. D. & Kannel, W. B. Atrial fibrillation as an independent risk factor for stroke: the Framingham Study. *Stroke* **22**, 983–988 (1991).
3. Wolf, P. A., D’Agostino, R. B., Kannel, W. B., Bonita, R. & Belanger, A. J. Cigarette smoking as a risk factor for stroke: the Framingham Study. *Jama* **259**, 1025–1029 (1988).
4. Tziomalos, K., Athyros, V. G., Karagiannis, A. & Mikhailidis, D. P. Dyslipidemia as a risk factor for ischemic stroke. *Curr. Top. Med. Chem.* **9**, 1291–1297 (2009).
5. Kurth, T. *et al.* Body mass index and the risk of stroke in men. *Arch. Intern. Med.* **162**, 2557–2562 (2002).
6. Xi, G., Keep, R. F. & Hoff, J. T. Mechanisms of brain injury after intracerebral haemorrhage. *Lancet Neurol.* **5**, 53–63 (2006).
7. Doyle, K. P., Simon, R. P. & Stenzel-Poore, M. P. Mechanisms of ischemic brain damage. *Neuropharmacology* **55**, 310–318 (2008).
8. Mozaffarian, D. *et al.* Heart disease and stroke statistics—2016 update: a report from the American Heart Association. *Circulation* **133**, e38–e360 (2016).
9. Bogousslavsky, J., Van Melle, G. & Regli, F. The Lausanne Stroke Registry: analysis of 1,000 consecutive patients with first stroke. *Stroke* **19**, 1083–1092 (1988).
10. Deb, P., Sharma, S. & Hassan, K. M. Pathophysiologic mechanisms of acute ischemic stroke: An overview with emphasis on therapeutic significance beyond thrombolysis.

Pathophysiology **17**, 197–218 (2010).

11. Jørgensen, H. S., Nakayama, H., Reith, J., Raaschou, H. O. & Olsen, T. S. Acute stroke with atrial fibrillation: the Copenhagen Stroke Study. *Stroke* **27**, 1765–1769 (1996).
12. Fisher, C. M. Lacunes: Small, deep cerebral infarcts. *Neurology* **77**, 2104 (2011).
13. Bamford, J., Sandercock, P., Jones, L. & Warlow, C. The natural history of lacunar infarction: the Oxfordshire Community Stroke Project. *Stroke* **18**, 545–551 (1987).
14. Vermeer, S. E., Longstreth Jr, W. T. & Koudstaal, P. J. Silent brain infarcts: a systematic review. *Lancet Neurol.* **6**, 611–619 (2007).
15. You, R., McNeil, J. J., O'malley, H. M., Davis, S. M. & Donnan, G. A. Risk factors for lacunar infarction syndromes. *Neurology* **45**, 1483–1487 (1995).
16. Jackson, C. A. *et al.* Differing risk factor profiles of ischemic stroke subtypes: evidence for a distinct lacunar arteriopathy? *Stroke* **41**, 624–629 (2010).
17. Simats, A., Garcia-Berrocso, T. & Montaner, J. Neuroinflammatory biomarkers: from stroke diagnosis and prognosis to therapy. *Biochim. Biophys. Acta (BBA)-Molecular Basis Dis.* **1862**, 411–424 (2016).
18. Turner, R. & Vink, R. Inhibition of neurogenic inflammation as a novel treatment for ischemic stroke. *Drug News Perspect* **20**, 221–226 (2007).
19. Jin, R., Yang, G. & Li, G. Inflammatory mechanisms in ischemic stroke: role of inflammatory cells. *J. Leukoc. Biol.* **87**, 779–789 (2010).
20. Schielke, G. P., Moises, H. C. & Betz, A. L. Blood to brain sodium transport and interstitial fluid potassium concentration during early focal ischemia in the rat. *J. Cereb.*

- Blood Flow Metab.* **11**, 466–471 (1991).
21. Lipton, S. A. & Rosenberg, P. A. Excitatory amino acids as a final common pathway for neurologic disorders. *N. Engl. J. Med.* **330**, 613–622 (1994).
 22. Yang, Y. & Rosenberg, G. A. Matrix metalloproteinases as therapeutic targets for stroke. *Brain Res.* **1623**, 30–38 (2015).
 23. Aoki, T., Sumii, T., Mori, T., Wang, X. & Lo, E. H. Blood-brain barrier disruption and matrix metalloproteinase-9 expression during reperfusion injury: mechanical versus embolic focal ischemia in spontaneously hypertensive rats. *Stroke* **33**, 2711–2717 (2002).
 24. Edvinsson, L. Cerebrovascular endothelin receptor upregulation in cerebral ischemia. *Curr. Vasc. Pharmacol.* **7**, 26–33 (2009).
 25. Zoppo, G. *et al.* Inflammation and stroke: putative role for cytokines, adhesion molecules and iNOS in brain response to ischemia. *Brain Pathol.* **10**, 95–112 (2000).
 26. Persson, M. G., Hedqvist, P. & Gustafsson, L. E. Nerve-induced tachykinin-mediated vasodilatation in skeletal muscle is dependent on nitric oxide formation. *Eur. J. Pharmacol.* **205**, 295–301 (1991).
 27. Kostulas, N., Pelidou, S. H., Kivisäkk, P., Kostulas, V. & Link, H. Increased IL-1 β , IL-8, and IL-17 mRNA expression in blood mononuclear cells observed in a prospective ischemic stroke study. *Stroke* **30**, 2174–2179 (1999).
 28. Gregersen, R., Lambertsen, K. & Finsen, B. Microglia and macrophages are the major source of tumor necrosis factor in permanent middle cerebral artery occlusion in mice. *J. Cereb. Blood Flow Metab.* **20**, 53–65 (2000).

29. Tian, X., Liu, C., Shu, Z. & Chen, G. Therapeutic Targeting of HMGB1 in Stroke. *Curr. Drug Deliv.* **14**, 785–790 (2017).
30. Mennicken, F., Maki, R., de Souza, E. B. & Quirion, R. Chemokines and chemokine receptors in the CNS: a possible role in neuroinflammation and patterning. *Trends Pharmacol. Sci.* **20**, 73–78 (1999).
31. Appay, V. & Rowland-Jones, S. L. RANTES: a versatile and controversial chemokine. *Trends Immunol.* **22**, 83–87 (2001).
32. Krupinski, J., Kumar, P., Kumar, S. & Kaluza, J. Increased expression of TGF- β 1 in brain tissue after ischemic stroke in humans. *Stroke* **27**, 852–857 (1996).
33. Van Exel, E. *et al.* Inflammation and stroke: the Leiden 85-plus study. *stroke* **33**, 1135–1138 (2002).
34. Giffard, R. G. & Yenari, M. A. Many mechanisms for hsp70 protection from cerebral ischemia. *J. Neurosurg. Anesthesiol.* **16**, 53–61 (2004).
35. Weise, J. *et al.* Deletion of cellular prion protein results in reduced Akt activation, enhanced postischemic caspase-3 activation, and exacerbation of ischemic brain injury. *Stroke* **37**, 1296–1300 (2006).
36. Yang, J.-T. *et al.* Dexamethasone inhibits ischemia-induced transient reduction of neurotrophin-3 mRNA in rat hippocampal neurons. *Neuroreport* **9**, 3477–3480 (1998).
37. Schäbitz, W.-R. *et al.* Neuroprotective effect of granulocyte colony--stimulating factor after focal cerebral Ischemia. *Stroke* **34**, 745–751 (2003).
38. DeGraba, T. J. *et al.* Increased endothelial expression of intercellular adhesion molecule-1

- in symptomatic versus asymptomatic human carotid atherosclerotic plaque. *Stroke* **29**, 1405–1410 (1998).
39. Stanimirovic, D. B., Wong, J., Shapiro, A. & Durkin, J. P. Increase in surface expression of ICAM-1, VCAM-1 and E-selectin in human cerebromicrovascular endothelial cells subjected to ischemia-like insults. in *Brain Edema X* 12–16 (Springer, 1997).
40. Radi, Z. A., Kehrli, M. E. & Ackermann, M. R. Cell adhesion molecules, leukocyte trafficking, and strategies to reduce leukocyte infiltration. *J. Vet. Intern. Med.* **15**, 516–529 (2001).
41. Hayashi, T., Noshita, N., Sugawara, T. & Chan, P. H. Temporal profile of angiogenesis and expression of related genes in the brain after ischemia. *J. Cereb. Blood Flow Metab.* **23**, 166–180 (2003).
42. Hara, A. *et al.* Immunohistochemical detection of Bax and Bcl-2 proteins in gerbil hippocampus following transient forebrain ischemia. *Brain Res.* **711**, 249–253 (1996).
43. Spite, M. & Serhan, C. N. Novel lipid mediators promote resolution of acute inflammation: impact of aspirin and statins. *Circ. Res.* **107**, 1170–1184 (2010).
44. Nathan, C. & Ding, A. Nonresolving inflammation. *Cell* **140**, 871–882 (2010).
45. Schilling, M. *et al.* Predominant phagocytic activity of resident microglia over hematogenous macrophages following transient focal cerebral ischemia: an investigation using green fluorescent protein transgenic bone marrow chimeric mice. *Exp. Neurol.* **196**, 290–297 (2005).
46. Denes, A. *et al.* Proliferating resident microglia after focal cerebral ischaemia in mice. *J.*

- Cereb. Blood Flow Metab.* **27**, 1941–1953 (2007).
47. Taylor, A., Verhagen, J., Blaser, K., Akdis, M. & Akdis, C. A. Mechanisms of immune suppression by interleukin-10 and transforming growth factor- β : the role of T regulatory cells. *Immunology* **117**, 433–442 (2006).
 48. Greenberg, D. A. & Jin, K. Growth factors and stroke. *NeuroRx* **3**, 458–465 (2006).
 49. Carmichael, S. T. Translating the frontiers of brain repair to treatments: starting not to break the rules. *Neurobiol. Dis.* **37**, 237–242 (2010).
 50. Hayakawa, K. *et al.* Inhibition of reactive astrocytes with fluorocitrate retards neurovascular remodeling and recovery after focal cerebral ischemia in mice. *J. Cereb. Blood Flow Metab.* **30**, 871–882 (2010).
 51. Zhang, Z. G. *et al.* Correlation of VEGF and angiopoietin expression with disruption of blood–brain barrier and angiogenesis after focal cerebral ischemia. *J. Cereb. Blood Flow Metab.* **22**, 379–392 (2002).
 52. Colton, C. A. *ponse* in the brain. *J. neuroimmune Pharmacol.* **4**, 399–418 (2009).
 53. Nowicka, D., Rogozinska, K., Aleksy, M., Witte, O. W. & Skangiel-Kramska, J. Spatiotemporal dynamics of astroglial and microglial responses after photothrombotic stroke in the rat brain. *Acta Neurobiol. Exp. (Wars).* **68**, 155 (2008).
 54. Abbott, N. J., Revest, P. A. & Romero, I. A. Astrocyte-endothelial interaction: physiology and pathology. *Neuropathol. Appl. Neurobiol.* **18**, 424–433 (1992).
 55. Dodson, R. F., Chu, L. W.-F., Welch, K. M. A. & Achar, V. S. Acute tissue response to cerebral ischemia in the gerbil: an ultrastructural study. *J. Neurol. Sci.* **33**, 161–170

- (1977).
56. Venero, J. L., Vizueté, M. L., Machado, A. & Cano, J. Aquaporins in the central nervous system. *Prog. Neurobiol.* **63**, 321–336 (2001).
 57. Ridet, J. L., Privat, A., Malhotra, S. K. & Gage, F. H. Reactive astrocytes: cellular and molecular cues to biological function. *Trends Neurosci.* **20**, 570–577 (1997).
 58. Rosenberg, P. A. & Aizenman, E. Hundred-fold increase in neuronal vulnerability to glutamate toxicity in astrocyte-poor cultures of rat cerebral cortex. *Neurosci. Lett.* **103**, 162–168 (1989).
 59. Vangeison, G. & Rempe, D. A. The Janus-faced effects of hypoxia on astrocyte function. *Neurosci.* **15**, 579–588 (2009).
 60. Pekny, M. & Lane, E. B. Intermediate filaments and stress. *Exp. Cell Res.* **313**, 2244–2254 (2007).
 61. Kim, J. S. Cytokines and adhesion molecules in stroke and related diseases. *J. Neurol. Sci.* **137**, 69–78 (1996).
 62. Tuttolomondo, A., Di Raimondo, D., di Sciacca, R., Pinto, A. & Licata, G. Inflammatory cytokines in acute ischemic stroke. *Curr. Pharm. Des.* **14**, 3574–3589 (2008).
 63. Orzyłowska, O., Oderfeld-Nowak, B., Zaremba, M., Januszewski, S. & Mossakowski, M. Prolonged and concomitant induction of astroglial immunoreactivity of interleukin-1beta and interleukin-6 in the rat hippocampus after transient global ischemia. *Neurosci. Lett.* **263**, 72–76 (1999).
 64. Lau, L. T. & Yu, A. C.-H. Astrocytes produce and release interleukin-1, interleukin-6,

- tumor necrosis factor alpha and interferon-gamma following traumatic and metabolic injury. *J. Neurotrauma* **18**, 351–359 (2001).
65. Fidler, P. S. *et al.* Comparing astrocytic cell lines that are inhibitory or permissive for axon growth: the major axon-inhibitory proteoglycan is NG2. *J. Neurosci.* **19**, 8778–8788 (1999).
 66. Lefrançois, T., Fages, C., Peschanski, M. & Tardy, M. Neuritic outgrowth associated with astroglial phenotypic changes induced by antisense glial fibrillary acidic protein (GFAP) mRNA in injured neuron–astrocyte cocultures. *J. Neurosci.* **17**, 4121–4128 (1997).
 67. Mun-Bryce, S. & Rosenberg, G. A. Matrix metalloproteinases in cerebrovascular disease. *J. Cereb. Blood Flow Metab.* **18**, 1163–1172 (1998).
 68. Rosenberg, G. A., Estrada, E. Y. & Dencoff, J. E. Matrix metalloproteinases and TIMPs are associated with blood-brain barrier opening after reperfusion in rat brain. *Stroke* **29**, 2189–2195 (1998).
 69. Nimmerjahn, A., Kirchhoff, F. & Helmchen, F. Resting microglial cells are highly dynamic surveillants of brain parenchyma in vivo. *Science* (80-.). **308**, 1314–1318 (2005).
 70. Deng, Y. Y., Lu, J., Ling, E. A. & Kaur, C. Monocyte chemoattractant protein-1 (MCP-1) produced via NF- κ B signaling pathway mediates migration of amoeboid microglia in the periventricular white matter in hypoxic neonatal rats. *Glia* **57**, 604–621 (2009).
 71. Davalos, D. *et al.* ATP mediates rapid microglial response to local brain injury in vivo. *Nat. Neurosci.* **8**, 752 (2005).

72. Taylor, R. A. & Sansing, L. H. Microglial responses after ischemic stroke and intracerebral hemorrhage. *Clin. Dev. Immunol.* **2013**, (2013).
73. Yenari, M. A., Kauppinen, T. M. & Swanson, R. A. Microglial activation in stroke: therapeutic targets. *Neurotherapeutics* **7**, 378–391 (2010).
74. Czeh, M., Gressens, P. & Kaindl, A. M. The yin and yang of microglia. *Dev. Neurosci.* **33**, 199–209 (2011).
75. Ponomarev, E. D., Veremeyko, T. & Weiner, H. L. MicroRNAs are universal regulators of differentiation, activation, and polarization of microglia and macrophages in normal and diseased CNS. *Glia* **61**, 91–103 (2013).
76. Crain, J. M., Nikodemova, M. & Watters, J. J. Microglia express distinct M1 and M2 phenotypic markers in the postnatal and adult central nervous system in male and female mice. *J. Neurosci. Res.* **91**, 1143–1151 (2013).
77. Vivien, D. & Ali, C. Transforming growth factor- β signalling in brain disorders. *Cytokine Growth Factor Rev.* **17**, 121–128 (2006).
78. Wycoco, V., Shroff, M., Sudhakar, S. & Lee, W. White matter anatomy: what the radiologist needs to know. *Neuroimaging Clin.* **23**, 197–216 (2013).
79. Pfeiffer, S. E., Warrington, A. E. & Bansal, R. The oligodendrocyte and its many cellular processes. *Trends Cell Biol.* **3**, 191–197 (1993).
80. Matute, C., Domercq, M., Pérez-Samartín, A. & Ransom, B. R. Protecting white matter from stroke injury. *Stroke* **44**, 1204–1211 (2013).
81. Weishaupt, N., Zhang, A., Deziel, R. A., Tasker, R. A. & Whitehead, S. N. Prefrontal

- ischemia in the rat leads to secondary damage and inflammation in remote gray and white matter regions. *Front. Neurosci.* **10**, 81 (2016).
82. Coleman, M. P. & Perry, V. H. Axon pathology in neurological disease: a neglected therapeutic target. *Trends Neurosci.* **25**, 532–537 (2002).
83. Dewar, D., Yam, P. & McCulloch, J. Drug development for stroke: importance of protecting cerebral white matter. *Eur. J. Pharmacol.* **375**, 41–50 (1999).
84. Thiel, A., Cechetto, D. F., Heiss, W.-D., Hachinski, V. & Whitehead, S. N. Amyloid burden, neuroinflammation, and links to cognitive decline after ischemic stroke. *Stroke* **45**, 2825–2829 (2014).
85. Xiong, X.-Y., Liu, L. & Yang, Q.-W. Functions and mechanisms of microglia/macrophages in neuroinflammation and neurogenesis after stroke. *Prog. Neurobiol.* **142**, 23–44 (2016).
86. Rosenberg, G. A. Inflammation and white matter damage in vascular cognitive impairment. *Stroke* **40**, S20–S23 (2009).
87. Pantoni, L., Garcia, J. H. & Gutierrez, J. A. Cerebral white matter is highly vulnerable to ischemia. *Stroke* **27**, 1641–1647 (1996).
88. Ho, P. W. *et al.* Is white matter involved in patients entered into typical trials of neuroprotection? *Stroke* **36**, 2742–2744 (2005).
89. Zhang, J., Zhang, Y., Xing, S., Liang, Z. & Zeng, J. Secondary neurodegeneration in remote regions after focal cerebral infarction: a new target for stroke management? *Stroke* **43**, 1700–1705 (2012).

90. Thiel, A. & Heiss, W.-D. Imaging of Microglia Activation in Stroke. *Stroke* **42**, 507–512 (2011).
91. Duering, M. *et al.* Acute infarcts cause focal thinning in remote cortex via degeneration of connecting fiber tracts. *Neurology* **84**, 1685–1692 (2015).
92. Weishaupt, N., Riccio, P., Dobbs, T., Hachinski, V. C. & Whitehead, S. N. Characterization of behaviour and remote degeneration following thalamic stroke in the rat. *Int. J. Mol. Sci.* **16**, 13921–13936 (2015).
93. Kurumatani, T., Kudo, T., Ikura, Y. & Takeda, M. White matter changes in the gerbil brain under chronic cerebral hypoperfusion. *Stroke* **29**, 1058–1062 (1998).
94. Debette, S. *et al.* Association of MRI markers of vascular brain injury with incident stroke, mild cognitive impairment, dementia, and mortality: the Framingham Offspring Study. *Stroke* **41**, 600–606 (2010).
95. Henninger, N. *et al.* Leukoaraiosis and sex predict the hyperacute ischemic core volume. *Stroke* **44**, 61–67 (2013).
96. Ay, H. *et al.* Severity of leukoaraiosis and susceptibility to infarct growth in acute stroke. *Stroke* **39**, 1409–1413 (2008).
97. Henninger, N., Khan, M. A., Zhang, J., Moonis, M. & Goddeau, R. P. Leukoaraiosis predicts cortical infarct volume after distal middle cerebral artery occlusion. *Stroke* **45**, 689–695 (2014).
98. Helenius, J. & Henninger, N. Leukoaraiosis burden significantly modulates the association between infarct volume and National Institutes of Health Stroke Scale in ischemic stroke.

- Stroke* **46**, 1857–1863 (2015).
99. Chaudhari, T. S. *et al.* Clinico-radiological predictors of vascular cognitive impairment (VCI) in patients with stroke: a prospective observational study. *J. Neurol. Sci.* **340**, 150–158 (2014).
 100. Curtze, S. *et al.* Cerebral computed tomography-graded white matter lesions are associated with worse outcome after thrombolysis in patients with stroke. *Stroke* STROKEAHA--115 (2015).
 101. Dacosta-Aguayo, R. *et al.* Structural integrity of the contralesional hemisphere predicts cognitive impairment in ischemic stroke at three months. *PLoS One* **9**, e86119 (2014).
 102. Podgorska, A., Hier, D. B., Pytlewski, A. & Czlonkowska, A. Leukoaraiosis and stroke outcome. *J. Stroke Cerebrovasc. Dis.* **11**, 336–340 (2002).
 103. Lawrence, A. J., Chung, A. W., Morris, R. G., Markus, H. S. & Barrick, T. R. Structural network efficiency is associated with cognitive impairment in small-vessel disease. *Neurology* **83**, 304–311 (2014).
 104. Rüber, T., Schlaug, G. & Lindenberg, R. Compensatory role of the cortico-rubro-spinal tract in motor recovery after stroke. *Neurology* **79**, 515–522 (2012).
 105. Chui, H. C. & Brown, N. N. Vascular cognitive impairment. *Contin. lifelong Learn. Neurol.* **13**, 109–143 (2007).
 106. Rincon, F. & Wright, C. B. Vascular cognitive impairment. *Curr. Opin. Neurol.* **26**, 29–36 (2013).
 107. Duering, M. *et al.* Identification of a strategic brain network underlying processing speed

- deficits in vascular cognitive impairment. *Neuroimage* **66**, 177–183 (2013).
108. Dichgans, M. & Leys, D. Vascular cognitive impairment. *Circ. Res.* **120**, 573–591 (2017).
109. Gonzalez, C. L. R. & Kolb, B. A comparison of different models of stroke on behaviour and brain morphology. *Eur. J. Neurosci.* **18**, 1950–1962 (2003).
110. Faraji, J., Lehmann, H., Metz, G. A. & Sutherland, R. J. Stress and corticosterone enhance cognitive recovery from hippocampal stroke in rats. *Neurosci. Lett.* **462**, 248–252 (2009).
111. Mok, V. C. T. *et al.* Cognitive impairment and functional outcome after stroke associated with small vessel disease. *J. Neurol. Neurosurg. Psychiatry* **75**, 560–566 (2004).
112. Elliott, R. Executive functions and their disorders: Imaging in clinical neuroscience. *Br. Med. Bull.* **65**, 49–59 (2003).
113. O’sullivan, M., Barrick, T. R., Morris, R. G., Clark, C. A. & Markus, H. S. Damage within a network of white matter regions underlies executive dysfunction in CADASIL. *Neurology* **65**, 1584–1590 (2005).
114. Seeley, W. W. *et al.* Dissociable intrinsic connectivity networks for salience processing and executive control. *J. Neurosci.* **27**, 2349–2356 (2007).
115. Kramer, J. H., Reed, B. R., Mungas, D., Weiner, M. W. & Chui, H. C. Executive dysfunction in subcortical ischaemic vascular disease. *J Neurol Neurosurg Psychiatry* **72**, 217–220 (2002).
116. Levit, A. *et al.* Behavioural inflexibility in a comorbid rat model of striatal ischemic injury and mutant hAPP overexpression. *Behav. Brain Res.* **333**, 267–275 (2017).
117. Monchi, O., Petrides, M., Petre, V., Worsley, K. & Dagher, A. Wisconsin Card Sorting

- revisited: distinct neural circuits participating in different stages of the task identified by event-related functional magnetic resonance imaging. *J. Neurosci.* **21**, 7733–7741 (2001).
118. Block, A. E., Dhanji, H., Thompson-Tardif, S. F. & Floresco, S. B. Thalamic--prefrontal cortical--ventral striatal circuitry mediates dissociable components of strategy set shifting. *Cereb. Cortex* **17**, 1625–1636 (2006).
119. Durukan, A. & Tatlisumak, T. Acute ischemic stroke: overview of major experimental rodent models, pathophysiology, and therapy of focal cerebral ischemia. *Pharmacol. Biochem. Behav.* **87**, 179–197 (2007).
120. Mhairi, M. I. New models of focal cerebral ischaemia. *Br. J. Clin. Pharmacol.* **34**, 302–308 (1992).
121. Traystman, R. J. Animal models of focal and global cerebral ischemia. *ILAR J.* **44**, 85–95 (2003).
122. Abe, K. *et al.* α -Tocopherol and ubiquinones in rat brain subjected to decapitation ischemia. *Brain Res.* **273**, 166–169 (1983).
123. Kofler, J. *et al.* Histopathological and behavioral characterization of a novel model of cardiac arrest and cardiopulmonary resuscitation in mice. *J. Neurosci. Methods* **136**, 33–44 (2004).
124. Herson, P. S. & Traystman, R. J. Animal models of stroke: translational potential at present and in 2050. *Future Neurol.* **9**, 541–551 (2014).
125. Robinson, R. G., Shoemaker, W. J., Schlumpf, M., Valk, T. & Bloom, F. E. Effect of experimental cerebral infarction in rat brain on catecholamines and behaviour. *Nature*

- 255, 332 (1975).
126. Belayev, L., Alonso, O. F., Busto, R., Zhao, W. & Ginsberg, M. D. Middle cerebral artery occlusion in the rat by intraluminal suture: neurological and pathological evaluation of an improved model. *Stroke* **27**, 1616–1623 (1996).
 127. Fluri, F., Schuhmann, M. K. & Kleinschnitz, C. Animal models of ischemic stroke and their application in clinical research. *Drug Des. Devel. Ther.* **9**, 3445 (2015).
 128. Li, F., Omae, T. & Fisher, M. Spontaneous hyperthermia and its mechanism in the intraluminal suture middle cerebral artery occlusion model of rats. *Stroke* **30**, 2464–2471 (1999).
 129. Purdy, P. D. *et al.* Microfibrillar collagen model of canine cerebral infarction. *Stroke* **20**, 1361–1367 (1989).
 130. Yang, Y., Yang, T., Li, Q., Wang, C. X. & Shuaib, A. A new reproducible focal cerebral ischemia model by introduction of polyvinylsiloxane into the middle cerebral artery: a comparison study. *J. Neurosci. Methods* **118**, 199–206 (2002).
 131. Kudo, M., Aoyama, A., Ichimori, S. & Fukunaga, N. An animal model of cerebral infarction. Homologous blood clot emboli in rats. *Stroke* **13**, 505–508 (1982).
 132. Ansar, S. *et al.* Characterization of a new model of thromboembolic stroke in C57 black/6J mice. *Transl. Stroke Res.* **5**, 526–533 (2014).
 133. Watson, B. D., Dietrich, W. D., Busto, R., Wachtel, M. S. & Ginsberg, M. D. Induction of reproducible brain infarction by photochemically initiated thrombosis. *Ann. Neurol.* **17**, 497–504 (1985).

134. Buchkremer-Ratzmann, I., August, M., Hagemann, G. & Witte, O. W.
Electrophysiological transcortical diaschisis after cortical photothrombosis in rat brain.
Stroke **27**, 1105–1111 (1996).
135. Dietrich, W. D., Busto, R., Watson, B. D., Scheinberg, P. & Ginsberg, M. D.
Photochemically induced cerebral infarction. *Acta Neuropathol.* **72**, 326–334 (1987).
136. Hughes, P. M. *et al.* Focal lesions in the rat central nervous system induced by endothelin-1. *J. Neuropathol. Exp. Neurol.* **62**, 1276–1286 (2003).
137. Sharkey, J. Perivascular microapplication of endothelin-1: a new model of focal cerebral ischaemia in the rat. *J. Cereb. Blood Flow Metab.* **13**, 865–871 (1993).
138. Roome, R. B. A model of Endothelin-1-mediated focal ischemia in the mouse forelimb motor cortex. (Memorial University of Newfoundland, 2013).
139. Soleman, S., Yip, P., Leasure, J. L. & Moon, L. Sustained sensorimotor impairments after endothelin-1 induced focal cerebral ischemia (stroke) in aged rats. *Exp. Neurol.* **222**, 13–24 (2010).
140. Carmichael, S. T. Rodent models of focal stroke: size, mechanism, and purpose. *NeuroRx* **2**, 396–409 (2005).
141. Roberts, B. W. & Trzeciak, S. Systemic inflammatory response after cardiac arrest: potential target for therapy? *Crit. Care Med.* **43**, 1336–1337 (2015).
142. Chastre, A. *et al.* Inflammatory cascades driven by tumor necrosis factor-alpha play a major role in the progression of acute liver failure and its neurological complications. *PLoS One* **7**, e49670 (2012).

143. Banks, P. A. *et al.* Classification of acute pancreatitis—2012: revision of the Atlanta classification and definitions by international consensus. *Gut* **62**, 102–111 (2013).
144. Gatson, J. W. *et al.* Estrogen treatment following severe burn injury reduces brain inflammation and apoptotic signaling. *J. Neuroinflammation* **6**, 30 (2009).
145. Reyes Jr, R. *et al.* Early inflammatory response in rat brain after peripheral thermal injury. *Neurosci. Lett.* **407**, 11–15 (2006).
146. Buras, J. A., Holzmann, B. & Sitkovsky, M. Model organisms: animal models of sepsis: setting the stage. *Nat. Rev. Drug Discov.* **4**, 854 (2005).
147. Szot, P. *et al.* Multiple lipopolysaccharide (LPS) injections alter interleukin 6 (IL-6), IL-7, IL-10 and IL-6 and IL-7 receptor mRNA in CNS and spleen. *Neuroscience* **355**, 9–21 (2017).
148. Ji, B., Higa, K., Soontornniyomkij, V., Miyanohara, A. & Zhou, X. A novel animal model for neuroinflammation and white matter degeneration. *PeerJ* **5**, e3905 (2017).
149. Pang, Y., Cai, Z. & Rhodes, P. G. Disturbance of oligodendrocyte development, hypomyelination and white matter injury in the neonatal rat brain after intracerebral injection of lipopolysaccharide. *Dev. Brain Res.* **140**, 205–214 (2003).
150. Lee, J.-C. *et al.* Accelerated cerebral ischemic injury by activated macrophages/microglia after lipopolysaccharide microinjection into rat corpus callosum. *Glia* **50**, 168–181 (2005).
151. Lehnardt, S. *et al.* The toll-like receptor TLR4 is necessary for lipopolysaccharide-induced oligodendrocyte injury in the CNS. *J. Neurosci.* **22**, 2478–2486 (2002).
152. Cai, Z., Pang, Y., Lin, S. & Rhodes, P. G. Differential roles of tumor necrosis factor- α

- and interleukin-1 β in lipopolysaccharide-induced brain injury in the neonatal rat. *Brain Res.* **975**, 37–47 (2003).
153. Cho, G.-S., Lee, J.-C., Ju, C., Kim, C. & Kim, W.-K. N-Methyl-D-aspartate receptor antagonists memantine and MK-801 attenuate the cerebral infarct accelerated by intracorpous callosum injection of lipopolysaccharides. *Neurosci. Lett.* **538**, 9–14 (2013).
 154. Pantoni, L. Cerebral small vessel disease: from pathogenesis and clinical characteristics to therapeutic challenges. *Lancet Neurol.* **9**, 689–701 (2010).
 155. Groenewegen, H. J. Organization of the afferent connections of the mediodorsal thalamic nucleus in the rat, related to the mediodorsal-prefrontal topography. *Neuroscience* **24**, 379–431 (1988).
 156. Schmahmann, J. D. Vascular syndromes of the thalamus. *Stroke* **34**, 2264–2278 (2003).
 157. Edelstyn, N. M. J., Mayes, A. R. & Ellis, S. J. Damage to the dorsomedial thalamic nucleus, central lateral intralaminar thalamic nucleus, and midline thalamic nuclei on the right-side impair executive function and attention under conditions of high demand but not low demand. *Neurocase* **20**, 121–132 (2014).
 158. Wang, X., Rousset, C. I., Hagberg, H. & Mallard, C. Lipopolysaccharide-induced inflammation and perinatal brain injury. in *Seminars in Fetal and Neonatal Medicine* **11**, 343–353 (2006).
 159. Floresco, S. B., Block, A. E. & Maric, T. L. Inactivation of the medial prefrontal cortex of the rat impairs strategy set-shifting, but not reversal learning, using a novel, automated procedure. *Behav. Brain Res.* **190**, 85–96 (2008).

160. Monaikul, S., Eubig, P., Floresco, S. & Schantz, S. Strategy set-shifting and response inhibition in adult rats exposed to an environmental polychlorinated biphenyl mixture during adolescence. *Neurotoxicol. Teratol.* **63**, 14–23 (2017).
161. Roof, R. L., Schielke, G. P., Ren, X. & Hall, E. D. A comparison of long-term functional outcome after 2 middle cerebral artery occlusion models in rats. *Stroke* **32**, 2648–2657 (2001).
162. Paxinos, G. & Watson, C. The rat brain in stereotaxic coordinates: hard cover edition. *Access Online via Elsevier* (2006).
163. Cordova, C. A., Jackson, D., Langdon, K. D., Hewlett, K. A. & Corbett, D. Impaired executive function following ischemic stroke in the rat medial prefrontal cortex. *Behav. Brain Res.* **258**, 106–111 (2014).
164. Langdon, K. D. *et al.* Executive dysfunction and blockage of brain microvessels in a rat model of vascular cognitive impairment. *J. Cereb. Blood Flow Metab.* 0271678X17739219 (2017).
165. Popa-Wagner, A., Buga, A.-M. & Kokaia, Z. Perturbed cellular response to brain injury during aging. *Ageing Res. Rev.* **10**, 71–79 (2011).
166. Popa-Wagner, A. *et al.* Accelerated infarct development, cytogenesis and apoptosis following transient cerebral ischemia in aged rats. *Acta Neuropathol.* **113**, 277–293 (2007).
167. Badan, I. *et al.* Accelerated glial reactivity to stroke in aged rats correlates with reduced functional recovery. *J. Cereb. Blood Flow Metab.* **23**, 845–854 (2003).

168. Castillo-Ruiz, M. M., Campuzano, O., Acarin, L., Castellano, B. & Gonzalez, B. Delayed neurodegeneration and early astrogliosis after excitotoxicity to the aged brain. *Exp. Gerontol.* **42**, 343–354 (2007).

Jessica R. Garabon

Curriculum Vitae

EDUCATION

Master of Science, Neuroscience
Western University, London, Ontario
September 2016-June 2018

Honours Bachelor of Science, Behaviour, Cognition, and Neuroscience with Distinction
University of Windsor, Windsor, Ontario
September 2012-April 2016

SCHOLARSHIPS AND BURSARIES

- | | |
|-----------|--|
| 2017 | Queen Elizabeth II Graduate Scholarship in Science and Technology:
Western University (\$15,000) |
| 2016 | Ontario Graduate Scholarship: Western University (\$15,000) |
| 2016 | Ontario Graduate Scholarship: University of Windsor (<i>Declined</i>)
(\$15,000) |
| 2016 | Natural Sciences and Engineering Research Council Canada Graduate
Scholarship – Master’s Program: University of Toronto (<i>Declined</i>)
(\$17,500) |
| 2016 | Libro Credit Union Student Award (\$3,000) |
| 2012-2016 | Renewable Entrance Scholarship: University of Windsor (\$6,400) |
| 2012 | Oshiomogho Atogwe I AM Foundation Scholarship (\$10,000) |
| 2012 | Harrow Booster Club Bursary (\$200) |
| 2012 | CAW Council Bursary (\$400) |

AWARDS AND HONOURS

- | | |
|------|--|
| 2016 | International Congress on the Biology of Fish Travel Award
Physiology Section of the American Fisheries Society (\$555 USD) |
|------|--|

- 2016 Franklin and Holder-Franklin Honours Project Award, Behaviour, Cognition, and Neuroscience Category 2nd Place
University of Windsor (\$50)
- 2016 People's Choice Award
UWill Discover Undergraduate Research Conference
University of Windsor (\$250)
- 2012-2016 Faculty of Science Dean's List
University of Windsor
- 2012 Ontario Scholar Achievement

RESEARCH EXPERIENCE

- 2016-Present Master of Science Candidate
Dr. Shawn Whitehead and Dr. Brian Allman, Western University
- 2016-Present Undergraduate Research Mentor
Dr. Shawn Whitehead, Western University
- 2016 Undergraduate Research Mentor
Dr. Dennis Higgs, University of Windsor
- 2016 Research Assistant
Dr. Dennis Higgs, University of Windsor
- 2015-2016 Undergraduate Honours Thesis Student
Dr. Dennis Higgs, University of Windsor
- 2014-2015 Sensory Biology Laboratory Volunteer Research Assistant
Dr. Dennis Higgs, University of Windsor

PUBLICATIONS

Garabon JR and Higgs DM (2017). The effects of stimulus parameters on auditory evoked potentials of *Carassius auratus*. *Journal of Comparative Physiology A*, 203(11), 945-951.

Levit A, Regis AM, **Garabon JR**, Oh SH, Desai S, Rajakumar N, Hachinski V, Agca Y, Agca C, Whitehead SN, Allman BL (2017). Behavioural flexibility in a comorbid rat model of striatal injury and mutant hAPP overexpression. *Behavioural Brain Research*, 333, 267-275.

CONFERENCE PRESENTATIONS

Snyder JR, Higgs DM. The effects of stimulus parameters on the evoked potentials of *Carassius auratus*. Presented at: 12th Annual International Congress on the Biology of Fish; June 12-16, 2016; San Marcos, TX.

Snyder JR, Higgs DM. The effects of stimulus parameters on the auditory brainstem response of *Carassius auratus*. Presented at: UWill Discover Undergraduate Research Conference; March 29, 2016; Windsor, ON.

Snyder JR, Higgs DM. The effects of stimulus parameters on the auditory brainstem response of *Carassius auratus*. Presented at: 29th Annual Ontario Biology Day; March 19-20, 2016; Toronto, ON.

Snyder JR, Allman BL, Whitehead SN. Correlating white matter changes with executive dysfunction in animal models of mediodorsal thalamic stroke and neuroinflammation. Presented at: London Health Research Day; May 10, 2018; London, ON.

Snyder JR, Allman BL, Whitehead SN. Correlating white matter changes with executive dysfunction in animal models of mediodorsal thalamic stroke and neuroinflammation. Presented at: Canadian Association of Neuroscience Annual Meeting; May 13-16 2018; Vancouver, BC.